

**Politecnico di Milano**

SCHOOL OF CIVIL, ENVIRONMENTAL AND LAND MANAGEMENT  
ENGINEERING  
MASTER OF SCIENCE IN HYDRAULIC ENGINEERING



MASTER'S DEGREE THESIS

**Testing a hydrological model on the  
Medellín river in Colombia**

*Supervisor*

Giovanni RAVAZZANI

*Assistant supervisor*

Lisdey Verónica HERRERA GÓMEZ

*Author*

Guglielmo ORSENIGO (919465)

A.Y. 2021/2022



# Abstract

The purpose of this thesis is the application of a hydrological model to improve the flood forecasting system of the metropolitan area of Aburrá valley in Columbia. The warning system is currently based on the observation and it's linked to the water exceeding the threshold water levels of the Medellín river, the alarm occurs only a few hours ahead of the event. Applying a hydrological model combined with a meteorological one would mean an important advance in alerting the responsible bodies and consequently it would allow the securing of people and goods with more effectiveness. The hydrological model applied is the *Flash-flood Event-based Spatially- distributed rainfall-runoff Transformation - Water Balance (FEST-WB)*, largely employed for the study of the hydrological balance and flood forecasting of alpine basins. The aim is to verify whether this model is also adaptable to basins with climatic and morphological features that differ from the usual field of application. The input operated is composed by meteorological and hydrological data measured by the *Sistema de Alerta Temprana de Medellín y el Valle de Aburrá (SIATA)*. This work represents a continuation of (Terbisi, 2021 [1])'s study which was a preliminary attempt of using the FEST-WB model on the Medellin river basin. The current analysis' result proves the suitability of the hydrological model for this kind of basin and, therefore, its employability for the flood forecasting and alert system in the area of interest which is often prone to hydraulic risks.

**Key words:** flood forecasting; hydrological model; FEST; warning system; Medellín; Colombia.



# Sommario

Lo scopo di questo lavoro è quello di testare un modello idrologico per potenziare il sistema di allertamento delle piene nella valle di Aburrà, in cui si espande l'area metropolitana della città di Medellín, in Colombia. Al momento, il piano emergenziale poggia interamente sul monitoraggio del livello del fiume, allertando in caso venga superata una determinata soglia. Ciò si traduce in un margine di azione di poche ore prima che la piena si verifichi. L'applicazione accoppiata di un modello idrologico con uno meteorologico accorcerebbe notevolmente i tempi di reazione, necessari agli enti responsabili, per garantire una messa in sicurezza di beni e persone che sia pronta ed efficace.

Il modello idrologico impiegato è il *Flash-flood Event-based Spatially-distributed rainfall-runoff Transformation - Water Balance (FEST-WB)*, notoriamente adoperato per la previsione delle piene in bacini alpini. L'obiettivo è verificare se tale modello sia adatto a studiare bacini con caratteristiche climatiche e morfologiche che si discostano dalle classiche condizioni di impiego. Gli input utilizzati sono dati meteorologici ed idrologici misurati sul campo dal *Sistema de Alerta Temprana de Medellín y el Valle de Aburrá (SIATA)*.

Questo lavoro rappresenta un proseguo dello studio fatto da (Terbisi, 2021 [1]), che mostra un tentativo preliminare di utilizzo del modello FEST-WB sul bacino del fiume Medellín. I risultati della corrente analisi provano quanto il modello idrologico sia adattabile a bacini di questo tipo e, quindi, utilizzabile per l'allertamento e la previsione delle piene nell'area in esame che spesso è soggetta a rischi idraulici.

**Parole chiave:** previsione delle inondazioni; modello idrologico; FEST; sistema di allerta; Medellín; Colombia.



# List of Figures

1.1	Examples of the effects of a flood during June 2021 in Antioquia. . . . .	2
2.1	Geographic context of the Aburrà valley. . . . .	8
2.2	Digital Elevation Model and hydrographic network. . . . .	9
2.3	Medellín river elevation profile. . . . .	10
2.4	Land cover map by ISCGM. . . . .	12
2.5	Soil clay content. . . . .	13
2.6	Soil sand content. . . . .	14
2.7	Soil silt content. . . . .	15
2.8	USDA Soil textural triangle. . . . .	15
2.9	Photos of rainfall events in Medellín. . . . .	17
2.10	Meteorological stations. . . . .	19
2.11	Velocity and water depth stations. . . . .	20
3.1	Hydrological cycle. . . . .	22
3.2	Scheme of the hydrological model FEST-WB. . . . .	23
3.3	Elaboration of temperature data. . . . .	24
3.4	Discretization scheme of the Muskingum-Cunge method. . . . .	28
3.5	<i>Aula Ambiental</i> cross section. . . . .	30
3.6	Station n.140 <i>Puente Fundadores</i> 's rating curve interpolated equation. . . . .	32
3.7	Discharge time series for St.99 - <i>Aula Ambiental</i> . . . . .	33
3.8	Discharge time series for St.106 - <i>Parque 3 Aguas</i> . . . . .	34
3.9	Discharge time series for St.169 - <i>La Clara</i> . . . . .	35
3.10	Discharge time series for St.140 - <i>Puente Fundadores</i> . . . . .	35
3.11	Discharge time series for St.260 - <i>Puente Gabino</i> . . . . .	35
3.12	Calibration: Flood event n.1. . . . .	39
3.13	Calibration: Flood event n.2. . . . .	39
3.14	Calibration: Flood event n.3. . . . .	40
3.15	Calibration: Flood event n.4. . . . .	40
3.16	Calibration: Flood event n.5. . . . .	40
3.17	Calibration: Flood event n.6. . . . .	41

3.18	Calibration: Flood event n.7. . . . .	41
3.19	Validation: Flood event n.1. . . . .	43
3.20	Validation: Flood event n.2. . . . .	43
3.21	Validation: Flood event n.3. . . . .	43
3.22	Validation: Flood event n.4. . . . .	44
3.23	Validation: Flood event n.5. . . . .	44
3.24	Validation: Flood event n.6. . . . .	44
3.25	Validation: Flood event n.7. . . . .	45
A.1	Parque 3 Aguas cross section. . . . .	54
A.2	Puente Fundadores cross section. . . . .	54
A.3	La Clara cross section. . . . .	55
A.4	Puente Gavino cross section. . . . .	55
B.1	Rating curve for the section Aula Ambiental. . . . .	58
B.2	Rating curve for the section Parque 3 Aguas. . . . .	58
B.3	Rating curve for the section La Clara. . . . .	59
B.4	Rating curve for the section Puente Gavino. . . . .	59

# List of Tables

- 2.1 Basin’s morphological characteristics. . . . . 11
- 2.2 Mean value of soil content . . . . . 13
  
- 3.1 Rating curve coefficients a and b for each of the five river sections  
analysed. . . . . 31
- 3.2 Catchment area values for each river section investigated. . . . . 33
- 3.3 Procedure of calibration: parameters and adaptation indexes. . . . . 38
- 3.4 Indexes for validation and calibration . . . . . 42



# Contents

List of figures	vii
List of Tables	ix
<b>1 Introduction</b>	<b>1</b>
1.1 Literature review . . . . .	3
1.2 Structure of the thesis . . . . .	5
<b>2 Study area</b>	<b>7</b>
2.1 Geographical and morphological overview . . . . .	7
2.2 Land cover . . . . .	11
2.3 Soil texture . . . . .	11
2.4 Climatic context . . . . .	16
2.5 Data network . . . . .	16
<b>3 Hydrological model</b>	<b>21</b>
3.1 Input data . . . . .	21
3.2 Water Balance . . . . .	25
3.3 Adjustment of the model . . . . .	29
<b>4 Conclusion</b>	<b>47</b>
<b>Bibliography and sitography</b>	<b>52</b>
<b>A HEC-RAS river cross sections</b>	<b>53</b>
<b>B Rating curves</b>	<b>57</b>



# Chapter 1

## Introduction

The several flood events registered in Colombia and, above all, the high quantity of damage to people and goods that these events caused, underlined the weakness in the approach to managing flood risks in the country. These events have also a negative effect on the economy and the ecology of Colombia. Indeed, every year the heavy rains lead to flooding of rivers and, consequently, landslides that cause dozens of deaths and thousands of displaced. Specifically from early March to the end of June of 2021, which corresponds approximatively to the first rainy season of the year, 74 deaths, 54 injured and 7 missing were reported. This was a consequence of the 1154 rainfall events occurred in 515 municipalities of the State [2]. In figure 1.1 are shown significant photos of the events of this period.

Currently, in Colombia, a uniformed flood forecasting system does not exist. Although a few warning schemes had been developed in selected basins by communities and local authorities, often these systems do not manage to give the warning in time. The present situation in Colombia is more or less the same as the one of the neighbouring countries. The biggest issue is the lack of a national authority that can coordinate and manage the implementation of the forecast model [3]. The meteorological condition of South-America complicates the situation because of its unpredictability, worsened by climate change.

A first attempt to understand whether the possibility to apply a model of flood forecast to a specific basin in Colombia exists has been developed by (Terbisi, 2021 [1]). Indeed, the risk given by the flood can be reduced thanks to the prediction of the event. This can reduce the part of the risk linked to the exposed elements and their vulnerability. A long term prediction of an overflow allows the responsible bodies to secure people and properties. It is fundamental to remind that the action of prediction of the critical events does not imply the elimination of the event but can be useful for the management of it.

Additionally, (Terbisi, 2021 [1]) reports the chance of a systematic measurement



(a) Flood in Santa Rosa de Osos - 15/06/2021 Photo: Dagrañ. [2]



(b) Flood in a street of Medellín - 11/06/2021  
Photo: Cortesía Denuncias Antioquia y Alcaldía  
de Medellín . [2]

Figure 1.1: Examples of the effects of a flood during June 2021 in Antioquia.

error for the starting data. As a matter of fact, the aim of this thesis is to try and adjust part of those data in order to see whether the hydrological model can actually work for the considered basin.

The area of study is the Aburrá valley in Antioquia department, it is the natural basin of river Medellín. The focus is on the Medellín city, the second-largest city of Colombia after Bogotá. The high level of urbanization causes frequent and dangerous floods. For this reason, the municipality of Medellín together with the public company EPM and the private one ISAGEN developed the Aburrá valley early warning system (SIATA) [4]. The aim of this system is to predict a natural event that can modify the environmental conditions of the area or that can be dangerous for the population. This operation is done starting from a solid real-time monitoring network.

The idea of applying a hydrological model to the basin is suggested by the disposability of high number of spatial and temporal data. In (Terbisi, 2021 [1]) the hydrological model used is the one called FEST-WB (Flash - flood Event - based Spatially distributed rainfall - runoff Transformation - Water Balance). FEST is a distributed model widely used in Italy; its output is the hydrogram computed for a certain river section, while the input consists of the rainfall and some descriptive parameters of the basin.

## 1.1 Literature review

River flooding currently impacts more people than any other environmental event posing a threat to almost 380 million urban residents globally [5]. During the last decades, extreme events have occurred with higher frequency due to climate change [6]. By combining this effect with the population growth and rapid urbanization, some countries will be more exposed to flood risk. Flood forecast event is central in the management of river flooding.

(Jain et al., 2018 [7]) present different aspect of flood forecasting and give a classification of model used for flood forecasting. The main subdivision is between stochastic and deterministic model. The first type simulate the random and probabilistic nature of inputs and responses that govern river flow. Deterministic models solve a set of equation representing the different watershed processes. These types of model can also be classified according to the spatial distribution of inputs and parameters. In lumped models, the catchment is idealized with various storage tanks, modelling consists in describe the movement of water through these tanks. In contrast, in a distributed model the catchment is divided into a large number of cells. Another important category is the model that use the concept of ensemble forecasting. The ensemble prediction systems offers an ensemble prediction of

hydrological variables. This result is obtained through small changes in the initial conditions, different representations of the physical processes and changes in parametrization and solution schemes.

(Alfieri et al., 2013 [8]) presents the Global Flood Awareness System (GloFAS), it is based on distributed hydrological simulation of numerical ensemble weather prediction with global coverage. Streamflow forecasts are compared statistically to climatological simulations to detect probabilistic exceedance of warning thresholds. River discharge is simulated by the Lisflood hydrological model for the flow routing in the river network and groundwater mass balance. Lisflood is a GIS-based spatially distributed hydrological model, which include a one-dimensional channel routing model (van der Knijff et al., 2010 [9]). The Lisflood model is currently running within the European Flood Alert System (EFAS).

(Thielen et al., 2009 [10]) presents the European Flood Alert System in which the ensemble of multiple hydrographs is analysed and combined to produce early flood warning information. EFAS is part of strategy for improved disaster management in Europe to reduce the impact of transnational floods through early warning. This can be achieved by providing National hydrological services with early flood information in addition to their own local and, mostly often, short-range forecasting information.

Flash floods are a recurrent hazard for many developing Latin American regions due to their complex mountainous terrain and the rainfall characteristics in the tropics [4].

(Domínguez-Calle and Lozano-Báez, 2014 [11]) does a review of the literature on the early warning systems for floods and droughts. It also presents early warning systems in Colombia. Event of La Niña in 2010 and 2011 caused economic loss, damage at the infrastructure and human losses, events of this size underlined lacks in the risk management and the necessity of early warning system in Colombia. The first system for risk management in Colombia was created in 1989 and was the SNGRD (Sistema Nacional de Gestión del Riesgo de Desastres). The first experience of the warning system was in 1976 through the SCMH (Servicio Colombiano de Hidrología y Meteorología). Currently the IDEAM (Instituto de Hidrología, Meteorología y Estudios Ambientales) presents a daily report of the hydrological warning and generates a public announcement for extraordinary events. This forecast system is based on the Water Research and Forecasting model (WRF) and on the V5 (MM5) model. Both the models use as initial conditions the data of the Global Forecast System (GFS, NOAA/NCEP, USA).

(López-García et al., 2015 [12]) review approaches to and field experiences with EWS (Early Warning System) throughout the world, including Colombia. They identified that many EWS are unimplemented; and once in operation, there exists an imbalance among components. On the other hand, some EWS fail to meet the

territory need as a result of poor community participation, both at design and operation stages.

(Ochoa Isaza, 2013 [13]) analyses the hydrological distributed model (SHIA) on the Medellín river in the Aburrá valley. This study is done with the aim of evaluating the impact of information that come from radar on the simulation. The distributed model SHIA is currently used in the early warning systems of Medellín in the Aburrá valley (SIATA).

On the same river (Medellín), (Terbisi, 2021 [1]) tries a first application of the distributed hydrological model FEST-WB. This was possible thanks to a large disposal of data, offered by the web portal SIATA, in terms of precipitation, temperature, water level, water velocity and geometry of many river bed cross sections. Nevertheless, it was not possible to adjust the model in the entire basin. This was due to the difficulty in understanding the value of discharge calculated through the measures of water depth and velocity [1]. The flow rate in some of the analysed sections seemed to be over-estimated [1]. (Terbisi, 2021 [1]) also suggests that the application of the model could be ameliorated computing the discharge without using the water velocity data. This would make possible to overcome the issue probably related to this type of measure. And that is exactly the path this thesis intends to pursue.

## 1.2 Structure of the thesis

Chapter 2 presents the study area with a geographical, morphological and climatic overview useful to understand the context in which the basin is inserted. Information about land cover and soil texture are also reported. At the end of the same chapter there is a description of the data network present in the Aburrá valley with a focus on the part used in this work.

In chapter 3 is presented the hydrological model, the main equations used by the model are reported. In its section 3.3 there is the application of the model and the results obtained.

In the last chapter (chapter 4) there are the discussion of the results and the possible future developments of the study.



# Chapter 2

## Study area

This chapter presents the basin under study. The main characteristics are reported, focusing attention on those that most influence the hydrological response of the basin. The information reported is the one of interest for the model and for the equations that are applied. The last part of the chapter describes the data network present in the basin.

### 2.1 Geographical and morphological overview

The area under consideration is the Aburrá Valley, in which is located the second biggest urban agglomeration of Colombia, for both population and economy. This valley is in the Antioquia Department, in the North West of Colombia (figure 2.1). The Aburrá Valley is located in the middle of Central Andes, therefore the territory is mountainous with irregular topography. Altitude is between 1300 and 2800 m a.s.l., the slope varies between 1-25% in 40% of the territory, 45% of the area has slightly steep terrain with slopes between 25-50% and the remaining 15% is steep with slopes that exceed 50%. The Digital Elevation Model is reported in figure 2.2, the dimensions of the cell are 200x200 metres. The urbanized area of the valley is the Metropolitan Area of the Aburrá Valley and rises in the flat area near the main river.

The valley under study constitutes the natural basin of the river Medellín which runs from South to North for 100 km. The watershed has an elongated shape in the north-east direction. The Medellín river originates in the south part of the basin, in the small town called Caldas, more specifically in the Alto de San Miguel at 2800 meters above sea level. The river runs through the entire valley to the limit of Barbosa town where it flows, together with the Rio Grande, into the Porce. In figure 2.2 the hydrographic network and the main reach can be seen. Medellín river is the main one, it cuts through the valley, the others rivers are all its

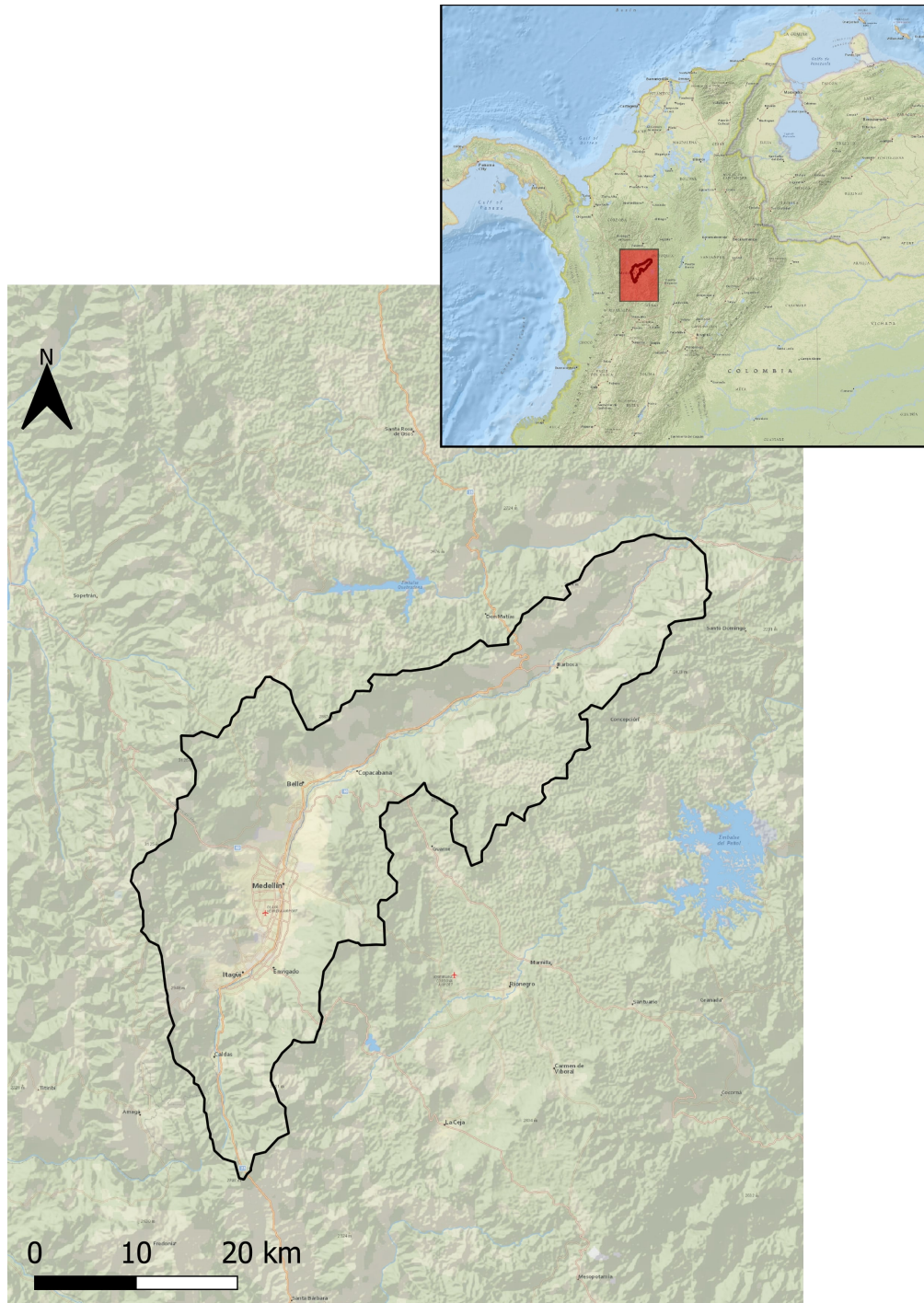


Figure 2.1: Geographic context of the Aburrà valley.

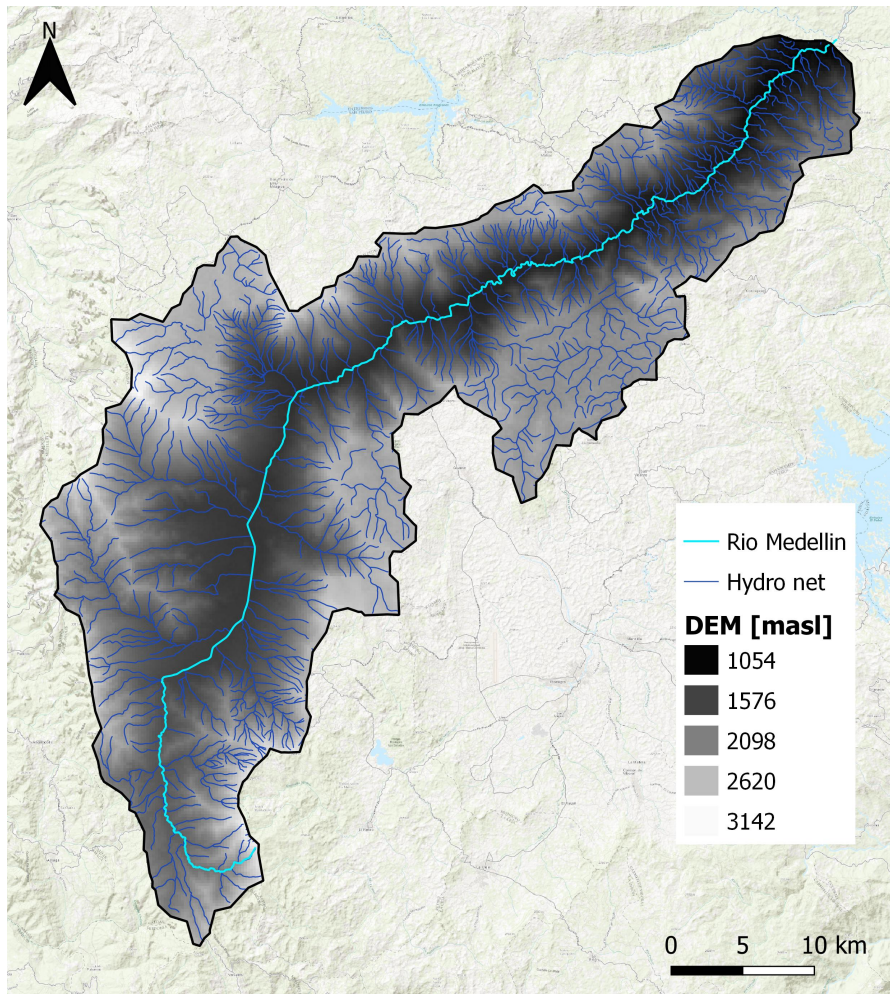


Figure 2.2: Digital Elevation Model and hydrographic network.

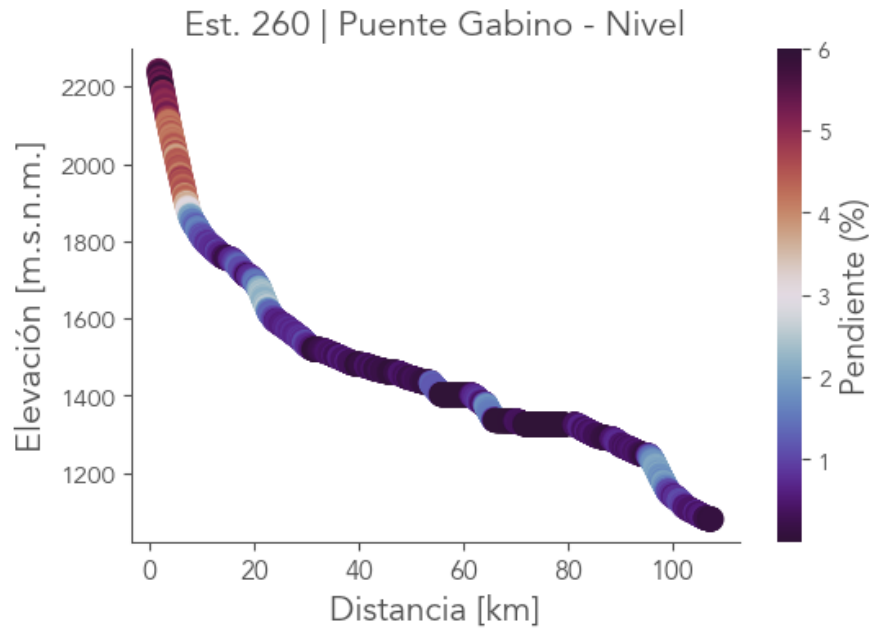


Figure 2.3: Medellín river elevation profile.

tributaries [13]. The hydrographic network reported comes from digitalization of physics maps. In figure 2.3 is reported the altitude profile of the river Medellín [4]. Some feature of the watershed are reported in table 2.1.

Along the main reach, there is only one deviation of the discharge. At the end of the river, between the municipalities of Barbosa and Santo Domingo, there is the hydroelectric power plant, Central Hidroeléctrica Carlos Lleras Restrep, it takes the waters through a spillway but it puts it back in the river. An additional discharge on the river, also located in the municipality of Barbosa, comes from La Tasajera hydroelectric power plant, which contributes, at most, with  $40 \text{ m}^3/\text{s}$ ; so, at the very end of the basin the discharge of Medellín includes also this value coming from another basin. Another power plant, sited in the region of Niquia, collects water from a different catchment area and offers an extra discharge of circa  $7 \text{ m}^3/\text{s}$  to to the river. This will be of fundamental importance when the analysis of the computed discharge time series is discussed. Given all the information above, it's clear that all the rainwater, which doesn't evaporate or filtrate deeply, joins the closing section of the basin. In general, the basin has a good capacity to keep the discharge, with a high and very high WRI (Water Retention Index) [14].

<b>Area [km<sup>2</sup>]</b>	1'218
<b>Mean altitude [m.a.s.m]</b>	1996
<b>Basin mean slope [%]</b>	22
<b>Main channel mean slope [%]</b>	0.72
<b>Main channel [km]</b>	107.67

Table 2.1: Basin's morphological characteristics.

## 2.2 Land cover

The territory analysed is located in the central Andes, has a latitude of 6 degrees north and reaches altitude of 2800 meters above sea level. These properties ensure that the basin is entirely covered by vegetation and the exclusion of the urban area that develops around the Medellín river. Figure 2.4 shows the land cover map produced by the ISCGM<sup>1</sup> [15]. The Global Land Cover by National Mapping Organizations classifies the status of the land cover into 20 categories. The classification is based on Land Cover Classification System (LCCS) developed by FAO. In the Aburrá valley, the non-urban areas are divided between forests and cultivated fields. The latter (in yellow in figure 2.4) is mostly located in the flattest areas of the basin and in its terminal part.

## 2.3 Soil texture

To study how the flow is created in the basin it is necessary to know some descriptive parameters of the soil. These are related to the texture of the soil, in fact, they are derived from empirical expressions knowing the type of soil.

Information about soil texture is available on the SoilGrids portal, a system for digital soil mapping based on a global compilation of soil profile data (WoSIS<sup>2</sup>) and environmental layers [16]. In figure 2.5, 2.6 and 2.7 are shown maps with the content of, respectively, clay, sand and silt at depth equal to 5/15 cm, the white parts are the urbanized area. The mean values of the three percentages are reported in table 2.2. Looking at these maps, it is possible to say that, in the entire basin there is the same texture. For this cause is reasonable to assume that, also under the urban area, there is the same soil texture.

Knowing percentages of silt, sand and clay is possible to obtain the soil type thanks to the USDA soil textural triangle (figure 2.8), this is the most simple and common way to classify soil [17]. The type of soil identify through the graph of the USDA classification, using the mean value of percentages of the content of sand,

<sup>1</sup>International Steering Committee for Global Mapping

<sup>2</sup>World Soil Information Service

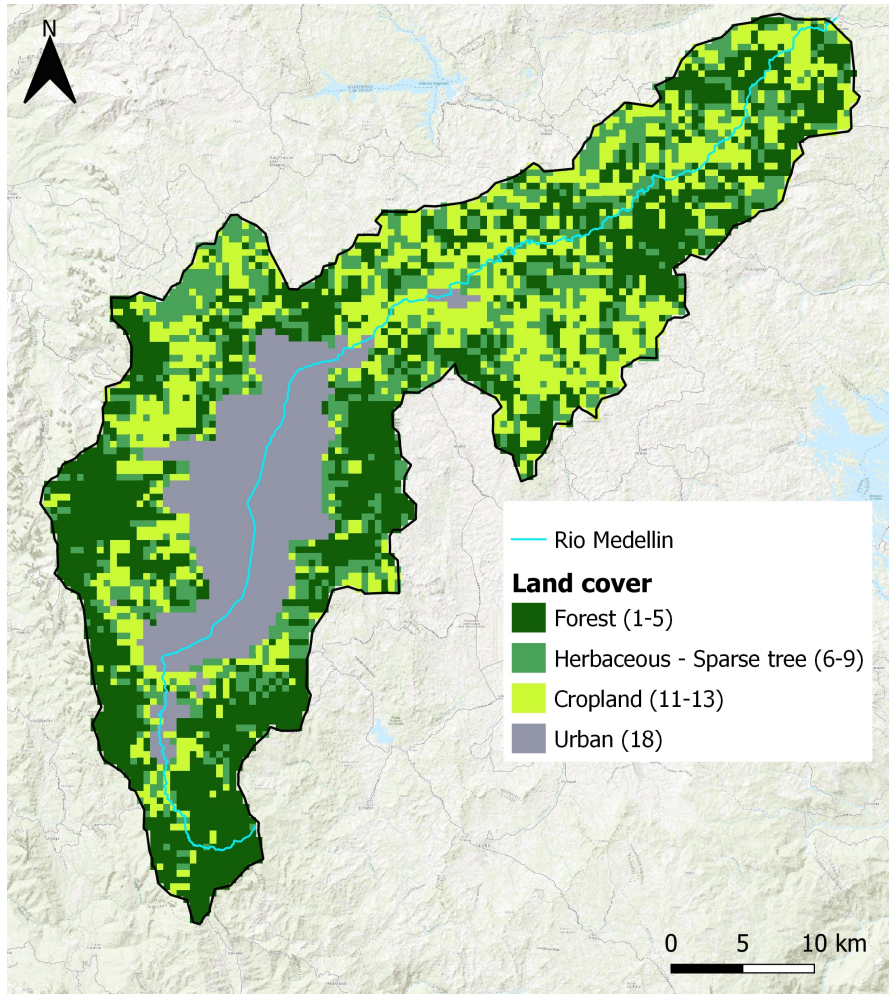


Figure 2.4: Land cover map by ISCGM.

silt and clay, is *Clay Loam*. This soil, in general, has the characteristics of clay but, in this case, the presence of silt and sand mitigate its features. Loams that contains clay tends to be heavy because of the density of clay. The density of the clay is the cause of the two biggest drawbacks of clay loam. When it is very wet, it swells to retains water, on the other hand, dry clay shrinks but stays packed, forming dense clods and cracking the soil surface.

	Mean content	
	[g/kg]	%
<b>Clay</b>	271.7	27.2
<b>Sand</b>	296.5	29.7
<b>Silt</b>	280.6	28.1

Table 2.2: Mean value of soil content

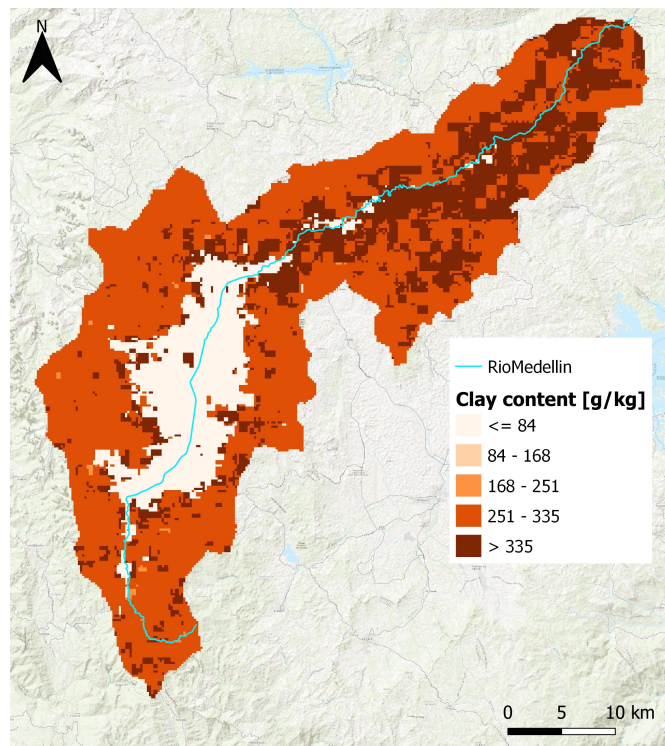


Figure 2.5: Soil clay content.

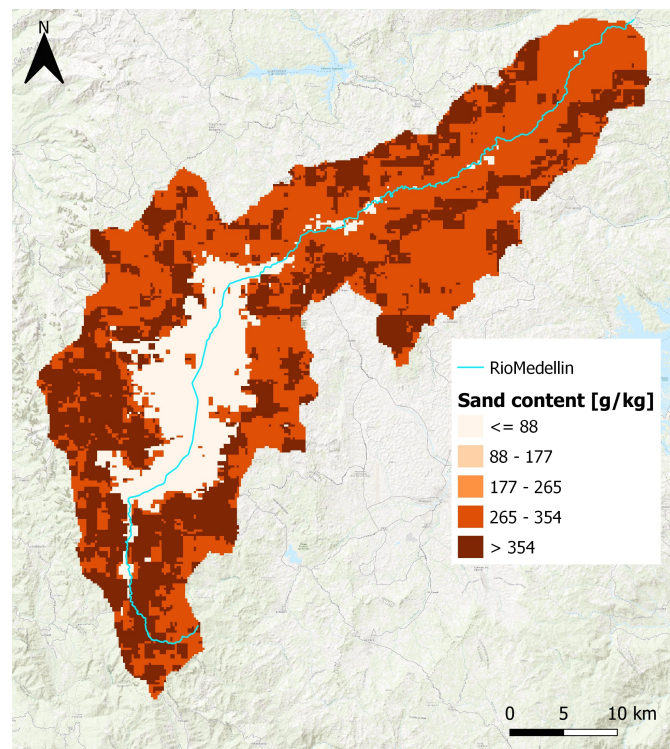


Figure 2.6: Soil sand content.

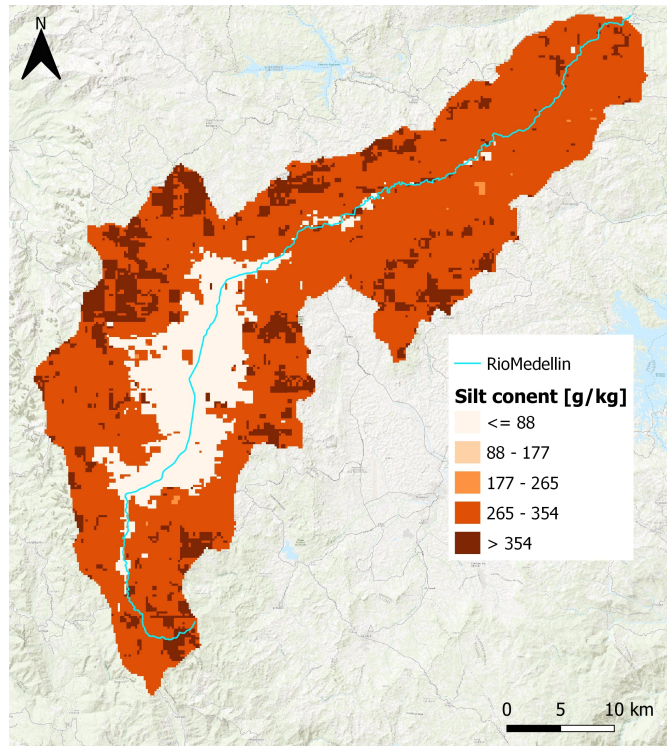


Figure 2.7: Soil silt content.

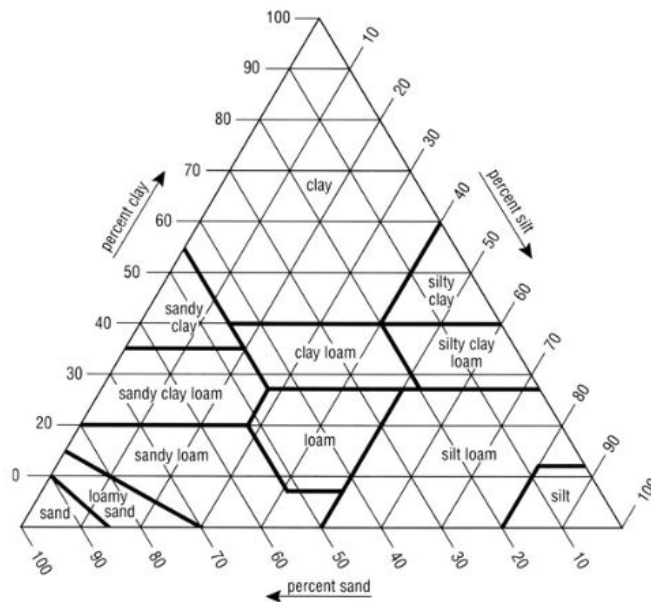


Figure 2.8: USDA Soil textural triangle.

## 2.4 Climatic context

The study area is classified, according to the Kröppen climate classification, as a tropical monsoon climate in the version of a less pronounced dry season. This means a climate almost uniform year-round. Thanks to the altitude of the valley, its climate is not as hot as other cities in the same latitude near the equator. The variation of temperature is limited, over the year there is about a constant temperature equal to 15/20°C. Albeit it's possible to identify two rainy seasons, there isn't a real dry season, rains are registers all over the year. The rainy intervals are March-April-May and September-October-November, these periods are characterized by a copious amount of rain usually in the form of frequent thunderstorms [13]. The mean precipitation changes with the altitude, in Medellín it can reach the values of 2630 *mm/year* [18]. Often the events are short but of high intensity and they are localized in a confined area. Since there are frequent rains when an event occurs the soil is already almost saturated so, the problem is to drain the rainwater. Photos in figure 2.9 are an example of the type of rainfall events in Medellín [19].

## 2.5 Data network

The watershed under study has a rich data network thanks to the system of early warning of Medellín and the Aburrá valley (SIATA). This system was established by the municipality of Medellín together with company EPM and ISAGEN. The main objectives of the project are real-time monitoring and early alerts. The network was activated in 2010 starting with 16 rainfall stations that measured the millimetres of precipitation with an interval of five minutes. Over the years it has developed by measuring different types of parameters both with remote sensing and with sensors located on the territory. Since 2013, the time interval has been reduced to one minute.

As a part of this thesis a small part of the monitoring network was used, specifically, the meteorological and the hydrological ones. The meteorological network includes sensors for measuring precipitation, temperature, pressure, wind speed, humidity and solar radiation. For the application of the hydrological model FEST, only precipitation and temperature data were collected. That is because measures of other quantities are too recent, so they don't provide a sufficient amount of data to do the hydrological simulation. The hydrological network measures the surface velocity and the water height of watercourses. These measurements are combined with the survey of the cross sections where the sensors are placed. [4]



(a) Medellín, 05 April 2021. [20]



(b) Medellín, 24 December 2020. [21]

Figure 2.9: Photos of rainfall events in Medellín.

## Meteorological network

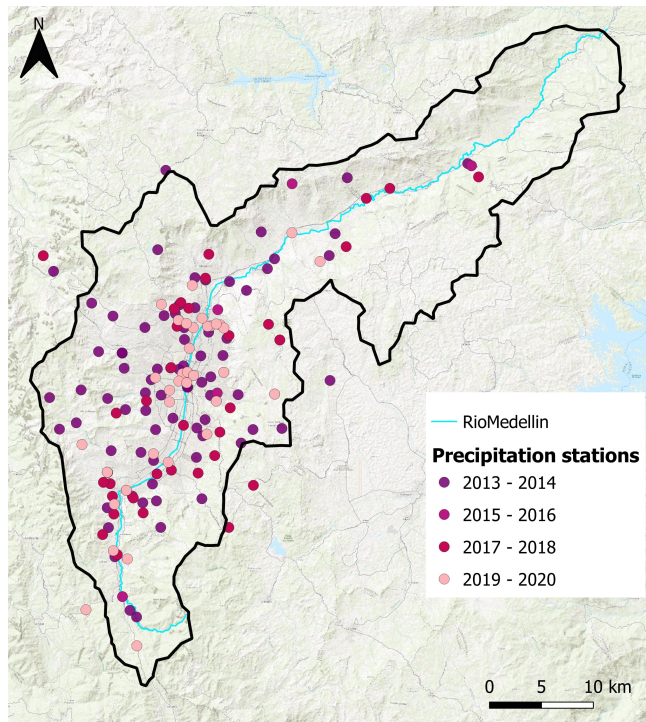
Rainfall is measured principally through pluviometers, that produce a value in *mm* of the depth of the precipitation that occurs over an unit of area in one minute. Other sensors to measure rain are disdrometers and meteorological sensors. The first one gives the amount of rainfall through measures of diameter and velocity of drops. The second type of sensor is a multiparametric one that provides information about precipitation, temperature, relative humidity, atmospheric pressure and wind velocity and direction.

On the territory the total amount of stations that can register precipitation is 224. However, some of them were not considered in this paper because they are too far from the basin under study or are activated only from a few months. The location of the 167 sensors take into account is shown in figure 2.10a. Some of the station examined are out of the basin but they are useful to recreate the precipitation in the area with only few sensors.

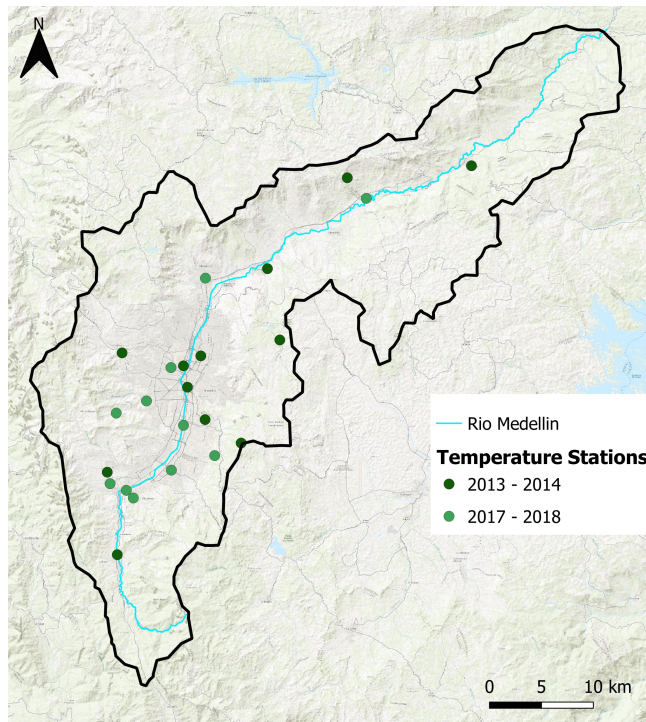
The same observation is valid for the temperature stations, in this case the total amount of sensors is 44 but only 24 are been considered. The location of the stations take analysed is reported in 2.10b. The scale color of the sensors in figure 2.10 depends on the date of activation, the lighter ones have been in operation for less time.

## Hydrological network

From hydrological network were used sensors for the measurement of water depth. This quantity is useful to calculate the discharge. In each station taken into account is important that, for at least a period of time, are present measures of water depth. The instruments are electromagnetic and measure the distance from the free surface. Some instruments use electromagnetic waves while others use ultrasonic. The position of the stations for the water depth measure are strategical because some of them are monitored for the early alert. Sound alarms are activated when the free surface reaches a certain level. This system allows the risk management stakeholders to evacuate the community. Albeit the network for the measurement of the water depth is very rich (88 stations), only 19 stations measure also the superficial velocity of the rivers and which 7 of the velocity stations have a significant amount of data since were installed before 2019. This was the reason that led (Terbisi, 2021 [1]) to work only with those 7 stations. As a matter of fact, (Terbisi, 2021 [1]) used both water level and water velocity in its study. In this thesis, as mentioned above, water velocity measurements won't be needed. However, the purpose of the present study is to be a follow up of (Terbisi, 2021 [1]), that's why both the stations and the time window of focus will be kept



(a) Precipitation measurement stations.



(b) Temperature measurement stations.

Figure 2.10: Meteorological stations.

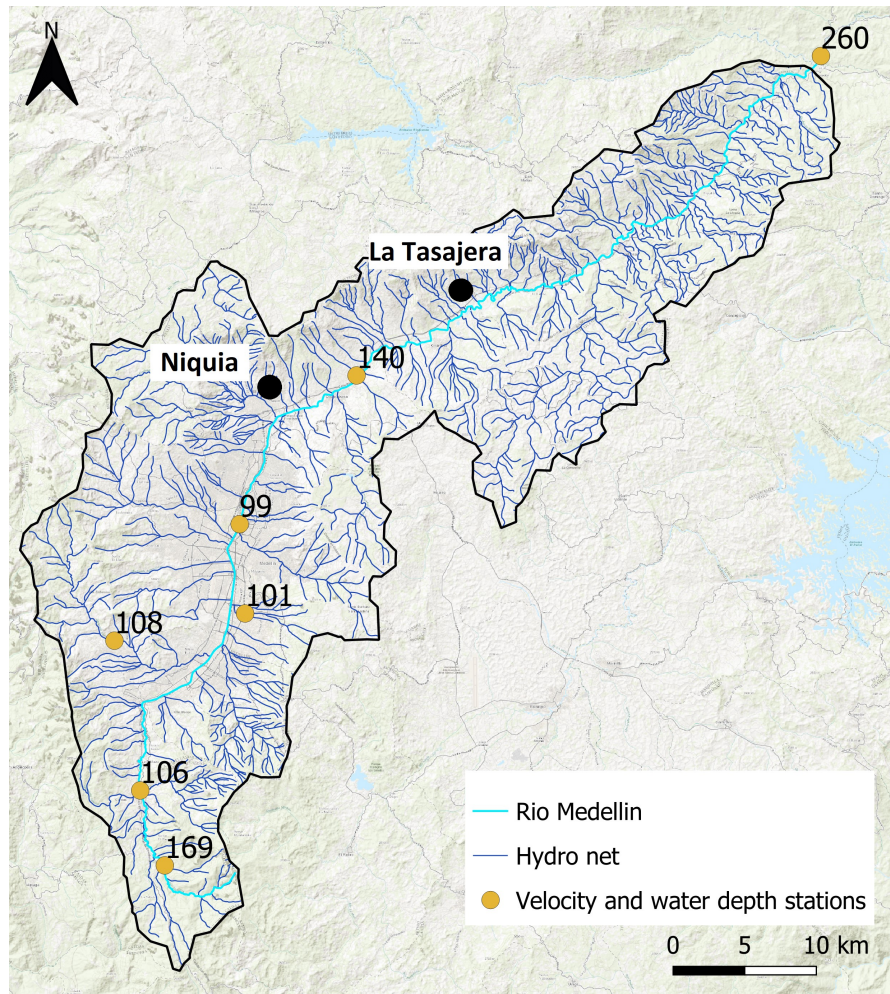


Figure 2.11: Velocity and water depth stations.

unchanged. Nonetheless, this study wants to focus on the main channel, while two of the stations are located on two different tributaries of Medellín, as it's shown in figure 2.11. As a result, this analysis considers only the five remaining river sections.

# Chapter 3

## Hydrological model

In this work the hydrological simulations are done with the model FEST-WB (Flash-flood Event-based Spatially-distributed rainfall-runoff Transformation - Water Balance) [22] [23] [24], a distributed hydrological continuous water balance model developed on the event based model FEST. Starting from the atmospheric forcing and soil parameters FEST-WB computes the outflow hydrograph through a water balance that considers the main processes of the hydrological cycle: evapotranspiration, infiltration, surface runoff, subsurface flow and snow dynamics (figure 3.1). In figure 3.2 there is a diagram of the model [25].

The FEST-WB model is classified as a distributed physic-based model. A physical based model is the one that applies the water balance considering the real hydrological dynamics and physical parameters that describe the basin. Distributed means that the spatial variation of the physical parameters, which describe the basin, is considered and therefore the computational domain is discretized with a mesh of regular square cells in each of which the water balance is calculated. Indeed, the value of the parameters and input data are given as a grid, value for each cell. Spatial variability is better considered with a more fine discretization, this, however, increases the calculation time.

### 3.1 Input data

The inputs of the model are meteorological forcing and grid maps of elevation and soil parameters.

The meteorological data depends on the equations used in the model, for this work the chosen formulas require only precipitation and temperature as input. The two variables are available in the portal of SIATA [4], in which the data is published every month. These data have been elaborated to create the input of the model. It consists of a file in which are assembled other files for every month

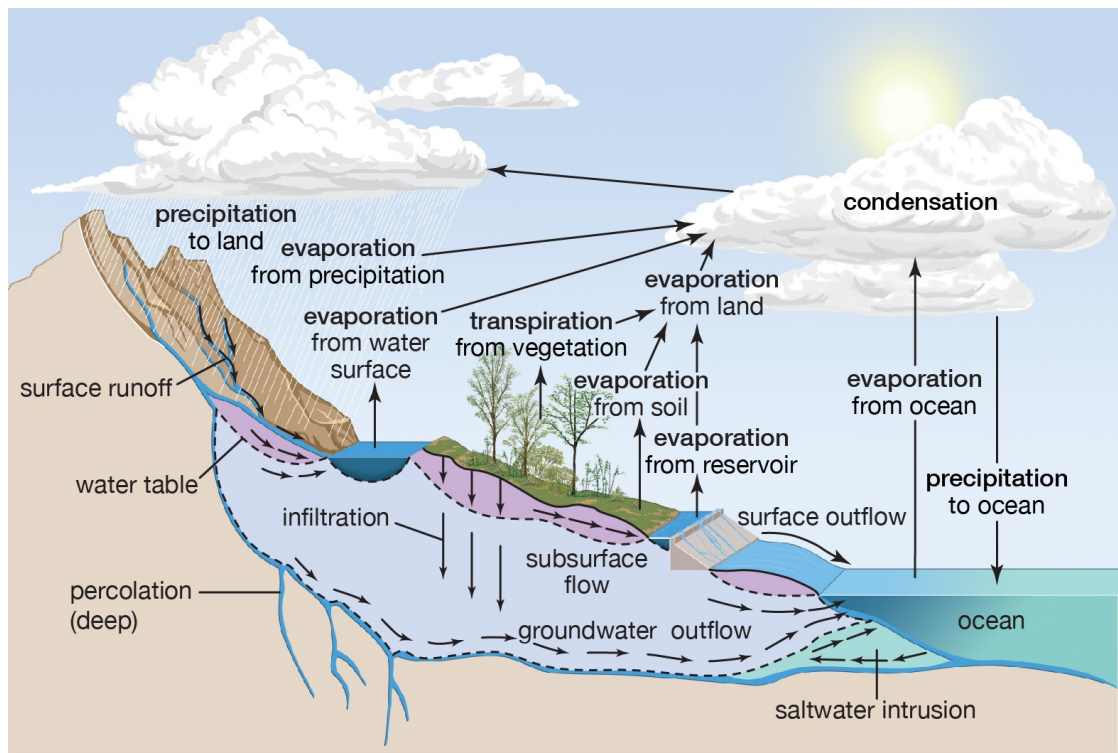


Figure 3.1: Hydrological cycle.

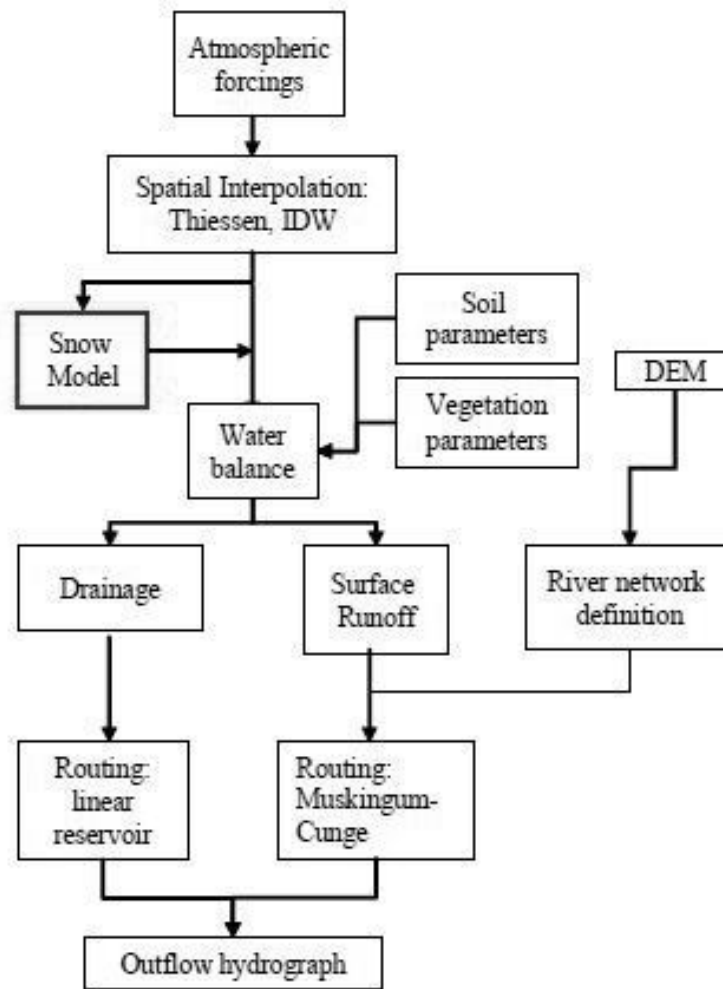


Figure 3.2: Scheme of the hydrological model FEST-WB.

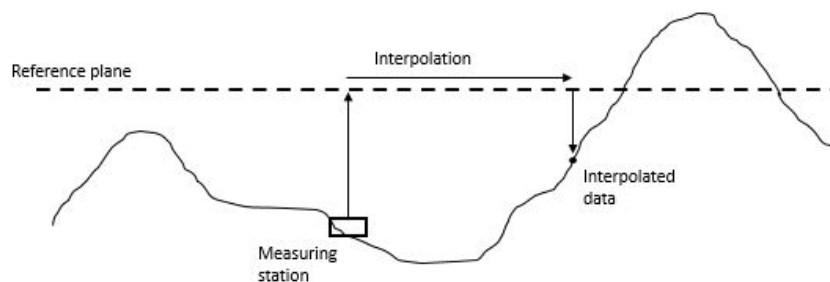


Figure 3.3: Elaboration of temperature data.

from 2013 to 2020 and for every station. These data are punctual and stations haven't the same date of installation (figure 2.10). The model applies interpolation to find a value for each cell of the basin from January 2013 to December 2020, of course, the interpolation is more accurate where there is a high concentration of old station. Measures are interpolated using the inverse distance weighting algorithm (IDW). Furthermore, the temperature changes also with altitude so it needs another interpolation. In the model a constant lapse rate adjusts the temperature for elevation, the average thermal gradient applied is  $-0.0065\text{ }^{\circ}\text{C}/\text{m}$ . Operations on temperature consist to scale the measured data into a reference plane with constant altitude, interpolate the data with IDW on this plane and then bring the interpolated data on the ground, in figure 3.3 is described this process. Thermal inversion phenomena are neglected. The results are two maps of cells  $200 \times 200$  metres with an interpolated value in each cells.

Digital Elevation Model (DEM) is an essential input for the model, in each cell of this map is reported the mean altitude of the cell. The map with the flow path network is automatically derived from the DEM, the procedure consists in assigning flow from each pixel to one of its eight neighbours. From the DEM are also obtain the hillslope and the channel network; the method to do this is to select a constant critical support area that defines the minimum drainage necessary to initiate a channel. The model, in this way, defines two types of cell, channel cells that drain an area greater than the critical one and other cells. Maps with descriptive parameters of the soil are also required. In this case of study, these features are inferred from the type of soil that is the same throughout basin (section 2.3). The input is therefore a map with values from which it is possible to identify the type of soil and, consequently, the descriptive parameters. This map contains the same value for each cells. The parameters used to describe the soil are the following:

- saturated conductivity ( $k_{sat}$  [ $\text{m}/\text{s}$ ]);
- saturated and residual volumetric water content ( $\theta_{sat}$ ,  $\theta_r$  [ $\text{m}^3/\text{m}^3$ ]);

- Brooks and Corey pore size distribution index ( $B$  [-]) and tortuosity index [-];
- bubbling pressure [m];
- field capacity and wilting point ( $\theta_{lim}$ ,  $\theta_{wp}$  [ $m^3/m^3$ ]);
- wetting front soil suction head [m];
- shape parameters of the retention function;
- initial abstraction and curve number value;
- storativity [mm] and maximum soil storage [m].

## 3.2 Water Balance

The FEST-WB model solves the water balance equation. Soil moisture ( $\theta$ ) evolution for the generic cell<sup>1</sup> at position  $i,j$  is described by water balance equation [23]:

$$\frac{\partial \theta_{i,j}}{\partial t} = \frac{1}{Z_{i,j}} (P_{i,j} - R_{i,j} - D_{i,j} - ET_{i,j}) \quad (3.1)$$

where  $P$  is precipitation rate,  $R$  is surface runoff flux,  $D$  is drainage flux,  $ET$  is evapo-transpiration rate and  $Z$  is the soil depth. The quantity ( $P_{i,j} - R_{i,j}$ ) is equivalent to infiltration  $I_{i,j}$ . The equation (3.1) is solved in the active layer of the basin that need to be set in the model. Under this tier is consider the presence of an impermeable layer.

The next paragraphs describe the physical process and the equations that regulate the water balance.

### Drainage flux

The drainage or percolation flux ( $D$ ) is the vertical flux in the soil. This quantity can be calculated, for one cell of the domain, with the following equation [26]:

$$D_t = k_{sat} \left( \frac{\theta_t - \theta_r}{\theta_{sat} - \theta_r} \right)^{\frac{2+3B}{B}} \quad (3.2)$$

---

<sup>1</sup>Actually, the equation is applied only in the cell not covered by snow but, in this work, the snow dynamics isn't treat because in the basin snow doesn't exist. For more detail about snow dynamics see [23].

whereas  $k_{sat}$  is the vertical permeability of the saturated soil and  $B$  is the Brooks and Corey pore size distribution index. The term in brackets is called  $\Theta$  and is the normalized volumetric water content; it depends on saturated and residual volumetric water content (respectively  $\theta_{sat}$ ,  $\theta_r$ ) and on the water content at time  $t$  ( $\theta_t$ ) [27].

## Infiltration

The infiltration process refers to the water not intercepted by vegetation for example. The process ends when the rain rate exceeds the infiltration capacity of the soil (Hortonian runoff). There are several models that can describe this process: in the FEST-WB the most used is the SCS-CN method. However, in this work is used the Philip's model, according to Sovinco's thesis in which it emerges as the best among the other ones [28].

Philip's two-term model equation is an approximate solution of Richards' equation for a short infiltration time [29]. The limitation of this approximation is that it can only be applied to homogeneous soil with stagnant initial water content. This is because this model assumes that infiltration starts when there is a layer of water on the ground [30]. According to the Philip's model, cumulative infiltration ( $I$  [L]) is expressed as:

$$I(t) = St^{1/2} + k_{sat}t \quad (3.3)$$

where  $S$  [ $LT^{1/2}$ ] is the sorptivity and  $k_{sat}$  [ $LT^{-1}$ ] is the saturated hydraulic conductivity. Sorptivity is a physical quantity that measures the capacity of a porous medium to uptake or release water by capillarity. For this reason, the first term of the equation (3.3) dominates the process during the initial stage of infiltration. As infiltration proceeds, the soil begins to get saturated and the second term becomes progressively more important, in this phase the gravitation forces dominate the capillarity. [31]

The rate of infiltration is determined by differential equation (3.3):

$$\frac{dI}{dt} = \frac{1}{2}St^{-1/2} + k_{sat} \quad (3.4)$$

## Evapo-Transpiration

Evapo-Transpiration ( $ET$ ) is the exchange of mass and energy between the soil-water-vegetation system and the atmosphere.  $ET$  is the combination of two processes whereby water is lost from the soil surface ( $E$ ) and from the crop ( $T$ ).

Evaporation is the process in which liquid water is converted to water vapour and is removed from the evaporating surface. This surface can be, for example,

lakes, soil, pavements and wet vegetation. Transpiration consists in the vaporization of liquid water contained in plant tissues. The water is taken up from the aquifer by the roots and transported through the plant, then the vapour exchange with the atmosphere occurs on the leaves. The requirement energy is given by solar radiation and, to a lesser extent, by the air temperature. The driving force to remove water from surfaces is the difference between the water vapour pressure at the evaporating surface and the one of the atmosphere. The process slows down and stops as the air gradually becomes saturated. It's necessary to replace the humid air with drier air, this process is made possible by the wind. Hence, solar radiation, air temperature, air humidity and wind speed are important parameters in the evaporation process. In this work, however, due to lack of data, it is impossible to use these parameters. For this reason it is applied the Hargreaves and Samani equation in which the inputs are only minimum and maximum air temperature [32] [33].

The real evapo-transpiration is computed by the potential evapo-transpiration ( $ET_p$ ). It is the maximum quantity of water that can evaporate in the ideal condition, that is, in the state of infinite availability water. In reality, the soil has a humidity condition that limits evapo-transpiration.

Hargreaves and Samani formulation for potential evapo-transpiration is:

$$ET_{pot} = HC \cdot RA \cdot \left( \frac{T_{max} + T_{min}}{2} + HT \right) \cdot (T_{max} - T_{min})^{HE} \quad (3.5)$$

where  $RA$  is in the same unit of  $ET_p$  and it is the extraterrestrial radiation,  $HE$  in an empirical exponent and it is equal to 0.5, and  $T_{min}$ ,  $T_{max}$  are respectively the daily minimum and maximum temperature expressed in Celsius [34].

The effective evapo-transpiration ( $ET$ ) is the sum of the effective evaporation and the effective transpiration:

$$ET = E + T \quad (3.6)$$

Both terms can be evaluated as a fraction of the potential evapo-transpiration depending on the water content at time  $t$  and on the percentage of soil covered by vegetation ( $f_v$ ) or percentage of bare soil ( $1-f_v$ ):

$$\begin{aligned} E &= \alpha(\theta_t) ET_p (1 - f_v) \\ T &= \beta(\theta_t) ET_p f_v \end{aligned} \quad (3.7)$$

where  $\alpha$  and  $\beta$  are coefficients depending on humidity:

$$\begin{aligned} \alpha &= 0.082 \theta_t + 9.173 \theta_t^2 - 9.815 \theta_t^3 \\ \beta &= \frac{\theta_t - \theta_{wp}}{\theta_{lim} - \theta_{wp}} \end{aligned} \quad (3.8)$$

where  $\theta_{lim}$  and  $\theta_{wp}$  are parameters that define the state at which soil moisture becomes limiting and eventually causes vegetation to wilt and transpiration to cease, respectively [35] [26].

## Diffusion wave

The superficial runoff routing, throughout the hillslope and the river network, is performed via a diffusion wave scheme, based on Muskingum-Cunge method in its non-linear form with the time-variable celerity. The model computes the surface runoff in each cell and propagates it along any reach of the basin flow path. The method uses both temporal and spatial discretization. The space is subdivided into a section which length is  $\Delta s$ , that is equal to the distance, along the line of maximum slope, between two cells of the grid of the basin; the time subdivision is set during the configuration of the model. In figure 3.4 is reported a scheme of the discretization,  $Q_i$  is the inflow discharge in a single cell and  $Q_{i+1}$  is the outflow discharge.

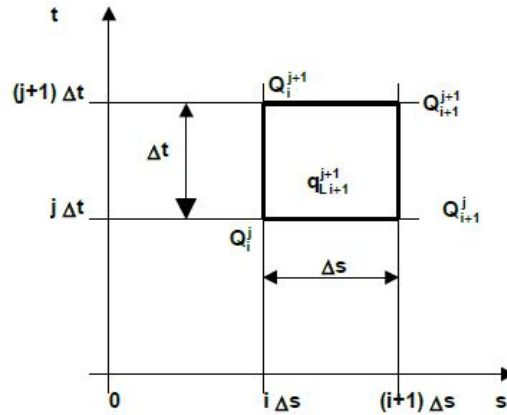


Figure 3.4: Discretization scheme of the Muskingum-Cunge method.

The routing scheme is given by:

$$Q_{i+1}^{j+1} = C_1 Q_i^{j+1} + C_2 Q_i^j + C_3 Q_{i+1}^j + q_{i+1}^{j+1} \quad (3.9)$$

where  $q_{i+1}^{j+1}$  is the lateral inflow rate to a cell of type channel;  $C_r$ , ( $r = 1, 2, 3$ ) are the routing coefficients and are obtained by using the continuity equation for the channel between the  $i$  and  $i+1$  nodes, and with the assumption that the storage volume  $W$  is a linear function of inflow and outflow discharge. Routing coefficients

are expressed as:

$$\begin{aligned} C_1 &= \frac{\Delta t - 2\tau\varepsilon}{2\tau(1 - \varepsilon) + \Delta t} \\ C_2 &= \frac{\Delta t + 2\tau\varepsilon}{2\tau(1 - \varepsilon) + \Delta t} \\ C_3 &= \frac{2\tau(1 - \varepsilon) - \Delta t}{2\tau(1 - \varepsilon) + \Delta t} \end{aligned} \quad (3.10)$$

where  $\tau$  is a coefficient related to the mean time taken by the wave to propagate along the channel and  $\varepsilon$  is a dimensionless weighting factor. The lateral inflow rate of the equation (3.9) is expressed as:

$$q_{i+1}^{j+1} = A_0 \frac{P_{e_{i-1}}^{j+1}}{\Delta t} \quad (3.11)$$

with  $P_{e_{i-1}}^{j+1}$  denoting direct runoff rate from the elemental cell  $i+1$  with area  $A_0$  as integrated in time from  $j\Delta t$  to  $(j+1)\Delta t$ . [36]

### 3.3 Adjustment of the model

A hydrological simulation system needs to be set for the study area. This procedure is divided into two parts: calibration and validation. Actually, there is a third part that is the initialization, the model needs this phase to determine some parameters and initial conditions for the simulation. As previously stated, the period of time taken in consideration is the same analysed by (Terbisi, 2021 [1]). Therefore, the inputs data of temperature and precipitation, measured per minutes, go from 1st January 2013 to 31th December 2020. The first year is used for the initialization, then the calibration is executed from January 2014 to December 2017 and the validation from January 2018 to December 2020. These processes consist in a comparison between the simulated superficial discharge with the FEST-WB model and the one calculated with the measured data.

In (Terbisi, 2021 [1]) the observed discharge was computed using measurements of water level and water velocity for all the sections mentioned. However, in some of those sections the obtained flow rate resulted to be unreasonably high with respect to their geometries and the dimensions of their catchment areas. This was probably due to an error during the assessment of the data. Even though it's impossible to know a priori which type of measured data contains an error, (Terbisi, 2021 [1]) suggests the problem is more likely to be found in the water velocity measurements. That's the reason why in this study the flow rate calculation is computed without utilizing that kind of information.

## Flow rate calculation

Since the values of discharge in the sections mentioned are not directly available, they need to be calculated through the data of water depth. They are computed with a time interval equal to 15 minutes because lower time intervals can cause instabilities in the FEST-WB model, generally it is used a bigger time interval but the nature of the event in this area suggests the use of small intervals.

The idea is to extract the rating curve equation that links the water depth with the discharge by means of the operating system HEC-RAS. Knowing the geometry, the slope and the Manning roughness coefficient of a river bed cross section, this software allows to generate flow profiles for as many discharge values as desired. Since the aim of this step is to obtain the rating curves for each section, uniform flow profiles for increasing equally spaced discharge values were created for each of the 5 sections.

As a representative example, figure 3.5 shows the cross section view of *Aula Ambiental* station offered by HEC-RAS after both the geometry and the Manning roughness coefficient were imported (Appendix A gathers the cross section view of the remaining 4 stations).

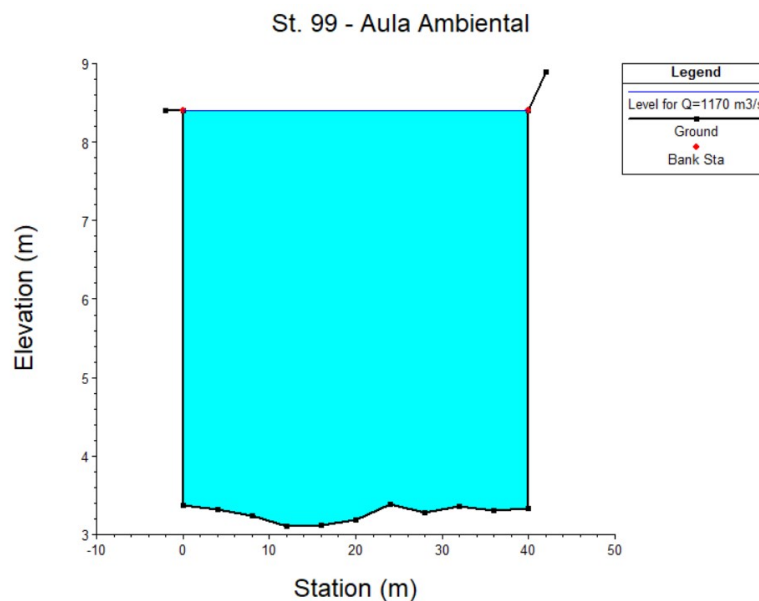


Figure 3.5: *Aula Ambiental* cross section.

The same picture also features, as a blue horizontal line, the highest possible water level simulated by the software which does not exceed the lowest of the two riverbanks, consequentially causing a flood over the surrounding area. Now it's possible to export the values of the not displayed water depths below the one just

detected, as well as the corresponding flow rates.

After putting these pairs of numbers on a graph with the water level and the flow rate as horizontal and vertical axes respectively, the interpolating equation of flow rate and water depth values is a power law in the form of:

$$Q = ah^b \quad (3.12)$$

Where the coefficients  $a$  and  $b$  are computed by means of the ordinary least square method. Table 3.1 reports the couples of these parameters obtained for each section, whereas in figure 3.6 it's pictured the interpolated flow rate equation regarding the *Puente Fundadores* station as an example. The other 4 rating curves are contained in Appendix B.

	<b>a</b>	<b>b</b>
<b>St. 99 - Aula Ambiental</b>	6.44E+01	1.77E+00
<b>St. 106 - Parque 3 Aguas</b>	2.31E+01	1.72E+00
<b>St. 140 - Puente Fundadores</b>	1.65E+01	1.92E+00
<b>St. 169 - La Clara</b>	1.12E+01	1.71E+00
<b>St. 260 - Puente Gabino</b>	2.63E+00	2.29E+00

Table 3.1: Rating curve coefficients  $a$  and  $b$  for each of the five river sections analysed.

The equations reconstructed are then applied to the water depth time series offered by SIATA in order to produce the corresponding discharge time series for the period going from January 2013 to December 2020. These series are portrayed in figures 3.7 to 3.11.

As far as river stations n.140 - *Puente Fundadores* and n.260 - *Puente Gabino* are concerned, in figures 3.10 and 3.11 it's easy to see the base flow is uncommonly high. It sets around  $45 \text{ m}^3/\text{s}$  in *Puente Fundadores* and it's about  $100 \text{ m}^3/\text{s}$  for *Puente Gabino*. Even though the location of these stations, especially section n.260, is much more downstream with respect to the other three and their geometries are greater, those flow rates seem to be still strangely excessive. This is justified by the presence of two hydroelectric power plants, *Niquia* and *La Tasajera* (see figure 2.11 in Chapter 2). Both of them, in fact, collect water from outside the Medellín river basin and then they channel that water volume in the Medellín river [37].

*Niquia* power plant is situated in the town of Bello, north side of the Abùrra valley, and its contribution to the the Medellín river in terms of flow rate is circa  $7 \text{ m}^3/\text{s}$ . This additional amount of water joins the natural river flow in an area that's downstream with respect to *Aula Ambiental* station, but upstream as for *Puente Fundadores* river section. This partially explains the  $30 \text{ m}^3/\text{s}$  difference

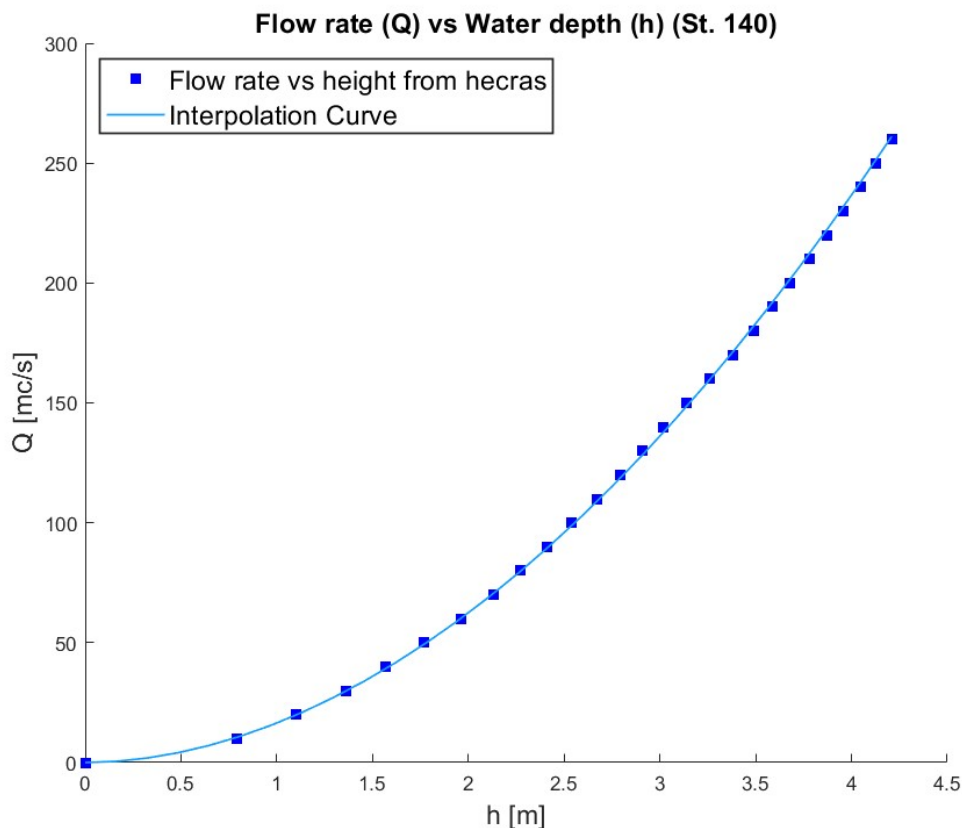


Figure 3.6: Station n.140 *Puente Fundadores*'s rating curve interpolated equation.

between the base river flow values registered in the two stations. It's reasonable to assume the rest of the extra discharge is linked to the increased catchment area being *Puente Fundadores* station around 20 km downstream. In table 3.2 the magnitudes of the five catchment areas are exposed.

The hydroelectric power plant of *La Tasajera* is also based in the northern side of the Aburrà valley, more specifically in the Barbosa district. This means it finds itself between St. n.140 and St. n.260. This underground power station adds approximately 40  $m^3/s$  to the stream flow. The ordinary flow rates of the two station differ from each other more or less by 50  $m^3/s$ . Supposing, as previously done for station 140, the remaining 10  $m^3/s$  are given by the enhancement of the catchment area, the discharge time series high values of both stations are thus justified.

The FEST-WB hydrological model is not able to take into consideration types of external contributes such as the one just discussed. Therefore *Puente Fundadores* and *Puente Gabino* river sections can't be employed during the calibra-

	Area [km <sup>2</sup> ]
St. 99 - Aula Ambiental	476
St. 106 - Parque 3 Aguas	98
St. 140 - Puente Fundadores	729
St. 169 - La Clara	26
St. 260 - Puente Gabino	1218

Table 3.2: Catchment area values for each river section investigated.

tion. Another section that can't be involved in the calibration procedure is *La Clara*, for the simple fact that there aren't water depth measurements available for the period of time covered by the process (January 2014 to December 2017). This means only *Aula Ambiental* and *Parque 3 Aguas* are going to be included in the next step of the analysis.

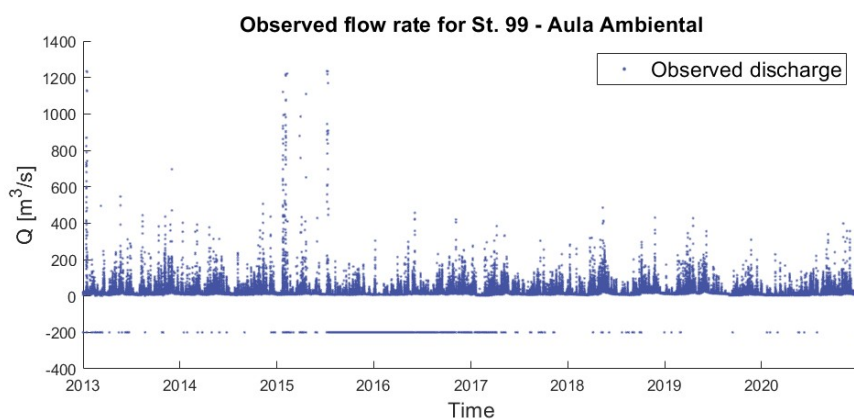


Figure 3.7: Discharge time series for St.99 - *Aula Ambiental*.

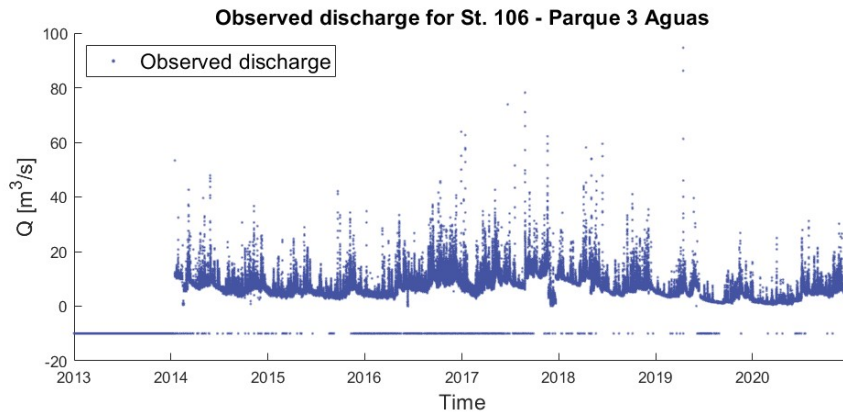
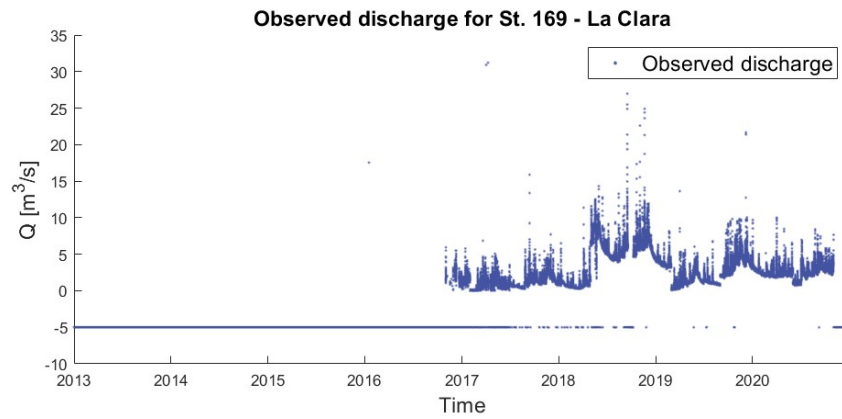
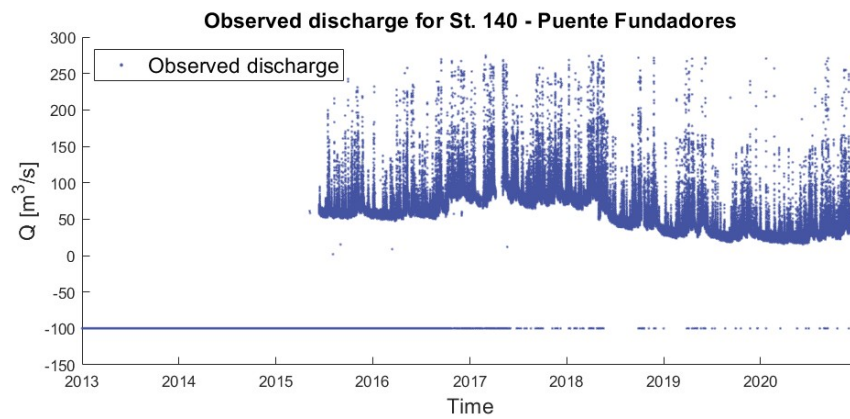
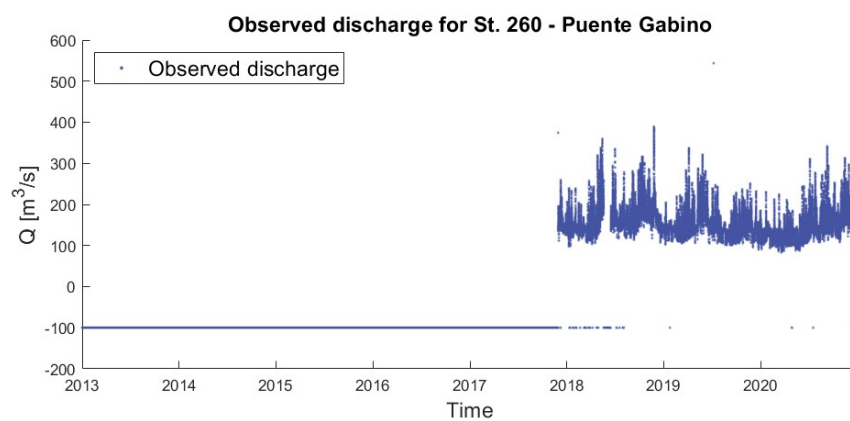


Figure 3.8: Discharge time series for St.106 - *Parque 3 Aguas*.

Figure 3.9: Discharge time series for St.169 - *La Clara*.Figure 3.10: Discharge time series for St.140 - *Puente Fundadores*.Figure 3.11: Discharge time series for St.260 - *Puente Gabino*.

## Calibration

The phase of calibration includes the modification of some parameters in the FEST-WB model in such a way that the simulated hydrograph of a flood event can resemble the respective observed one as good as possible. The calibration activity is based on the “trial and error” approach, this procedure consists of changing parameters until satisfying results are obtained [22]. In this way there is not unique solution because it’s possible to have more than one combination of parameters that optimize the solution.

The first thing to do is to pick out a bunch of significant flood events from the observed discharge time series. The episodes must be the same for the two stations examined. This choice is made excluding a priori flood events considered to be too extreme, thus unreliable for such a procedure. The 7 following flood events are the ones used to calibrate the model:

- Event n.1: started at 3:00 AM on the 21st of April 2014 and ended at 03:15 AM on the 23rd of April 2014;
- Event n.2: started at 3:15 AM on the 7th of May 2014 and ended at 05:45 AM on the 8th of May 2014;
- Event n.3: started at 4:15 AM on the 9th of November 2014 and ended at 11:30 PM on the 16th of November 2014;
- Event n.4: started at 5:15 AM on the 8th of December 2014 and ended at 08:45 AM on the 9th of December 2014;
- Event n.5: started at 00:15 AM on the 3rd of June 2016 and ended at 10:00 PM on the 5th of June 2016;
- Event n.6: started at 11:00 AM on the 5th of November 2016 and ended at 11:45 AM on the 6th of November 2016;
- Event n.7: started at 6:00 AM on the 8th of April 2017 and ended at 07:00 AM on the 9th of April 2017.

Looking at the flow rate trends observed in the two stations for the considered events, it’s instantly clear they have a different behaviour. This condition is caused by the fact that St. n.106 is located much upstream with respect to St. n.99, thus it’s possible that some precipitation events can happen to take place in the *Aula Ambiental* sub-basin, but not in the *Parque 3 Aguas* one. As a matter of fact, for the geographic area under investigation it’s not rare to spot rainfall events which are extremely condensed in a very small perimeter. The situation

illustrated above requires the calibration to be applied to only one of the two river sections. *Aula Ambiental* river station is placed in the middle of the urbanized area and that makes it more of interest for this type of study rather than *Parque 3 Aguas* station. This means St. n.99 alone is going to be the focus of this calibration phase from now on. Having defined the flood events, the adjustment of the parameters mentioned above is guided by the comparison between calculated values of discharge and the simulated ones. This is performed through some indexes that suggest the quality of the adaptation of the two data sets. The indexes investigated are four:

- Peak Discharge Relative Error [%]:

$$\varepsilon_{Q_{peak}} = \frac{(Q_{p,sim} - Q_{p,obs})}{Q_{p,obs}} \cdot 100 \quad (3.13)$$

where the subscripts *obs* and *sim* stand for "observed" and "simulated". The root mean square error can be between 0 and  $+\infty$ , a value equal to 0 means that the simulated flow rate corresponds to the calculated one.

- Root Mean Square Error [m<sup>3</sup>/s]:

$$RMSE = \sqrt{\frac{1}{n} \sum_{i=1}^n (Q_{obs}^i - Q_{sim}^i)^2} \quad (3.14)$$

where the subscript *obs* indicates the discharge calculated through observed variable. The root mean square error can be between 0 and  $+\infty$ , a value equal to 0 means that the simulated flow rate corresponds to the calculated one.

- Nash-Sutcliffe index:

$$E = 1 - \frac{\sum_{i=1}^n (Q_{obs}^i - Q_{sim}^i)^2}{\sum_{i=1}^n (Q_{obs}^i - \overline{Q_{obs}})^2} \quad (3.15)$$

this second index considers the quality of the simulation in respect to the mean of calculated values; it assumes values between  $-\infty$  and 1, if it is equal to 1 it means that there is a perfect representation of the phenomenon, if it is less than 0 than the mean of the calculated values is better than the simulated ones

- Mean bias:

$$\bar{\varepsilon} = \frac{1}{n} \sum_{i=1}^n (Q_{sim}^i - Q_{obs}^i) \quad (3.16)$$

it is the mean of the error of each value of  $Q$ , it is useful to understand if there is a underestimation ( $\bar{\epsilon} < 0$ ) or an overestimation ( $\bar{\epsilon} > 0$ )

Of the four indexes just reported, the Peak Discharge Relative Error is the only one used to lead the calibration process in this thesis. To be precise, its mean value among the 7 events is the guiding parameter. Namely its minimization represents the goal of the procedure.

The parameters modified during consecutive simulations are two:

- saturated conductivity  $k_{sat}$  [m/s] that is the vertical permeability that controls the infiltration and, therefore, the superficial flow rate; initially it is equal to the mean value for the type of soil present in the basin (clay loam):  $k_{sat} = 6.39 \cdot 10^{-7} \text{ m/s}$ ;
- Curve Number  $CN$  [-], a dimensionless coefficient which characterize the runoff properties of a soil; it can go from a value of zero, meaning the ground is completely permeable, to a maximum of 100, indicating a totally impervious surface. It's starting value here is 75.

In table 3.3 are reported the values of the parameters and the mean quantities of the adaptation indexes for each simulation. The best simulation is the number 4 (highlighted in green), which offers a peak discharge relative mean error equal to 5.19% . The 7 events considered are pictured in figures 3.12 to 3.18, the observed values are in black, while the red lines indicate the discharge functions generated by the chosen simulation (*Sim Finale*) and the green curves represent the first simulation of the flood episodes (*Sim 0*).

Sim.	$k_{sat}$ [m/s]	CN [-]	$\epsilon_{Q_{peak}}$ [%]	RMSE [m <sup>3</sup> /s]	E [-]	$\bar{\epsilon}$ [m <sup>3</sup> /s]
0	6.39E-07	75	-80.32	60.59	-0.18	-28.27
1	6.39E-08	75	-56.82	51.76	0.08	-20.84
2	6.39E-07	85	-49.17	51.18	0.03	-18.84
3	6.39E-07	92	-6.87	50.94	-0.14	-5.41
4	6.39E-07	93	5.19	54.81	-0.31	-2.61
5	6.39E-07	94	16.74	60.02	-0.56	0.53

Table 3.3: Procedure of calibration: parameters and adaptation indexes.

It's easy to notice the Curve Number is the most altered parameter. Its final value is indeed 93 which is very close to a impermeability condition. This has two justifications. First and foremost, St. n.99 is situated in the center of a widely urbanized area. This means a large part of its catchment area is actually impervious. In the second place, as mentioned before, the occurrence of spatially highly

concentrated rain events is not rare in this geographic area. So what happens is that big water volumes are poured on areas which can be around 1 – 2 *km* wide. This implies that those kind of precipitations are not captured by the pluviometers mesh, since it covers the ub-basin catchment area with a much looser net. Hence these undetected events are not counted as input for the model. To counterbalance this lack of records, it sounds logic to force the hydrological model by means of a greater value of the curve number.

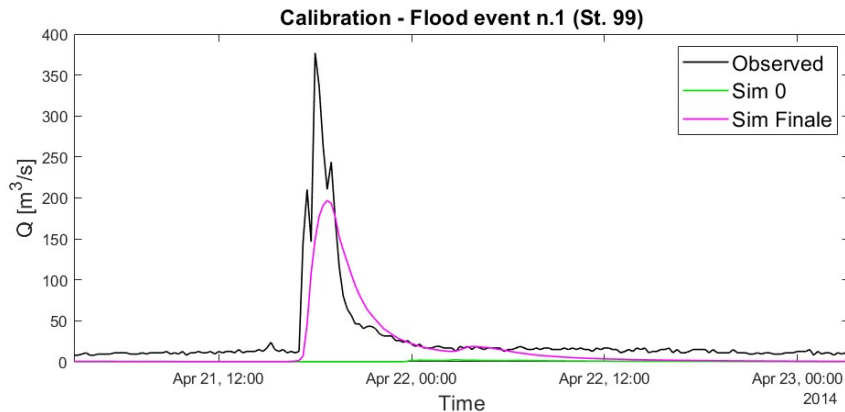


Figure 3.12: Calibration: Flood event n.1.

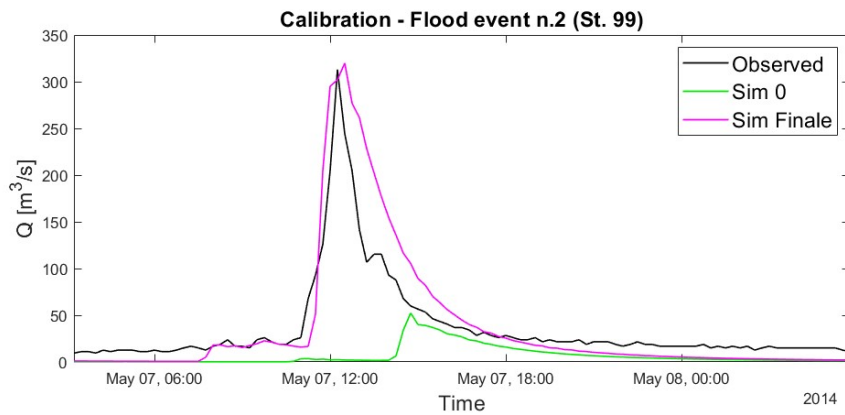


Figure 3.13: Calibration: Flood event n.2.

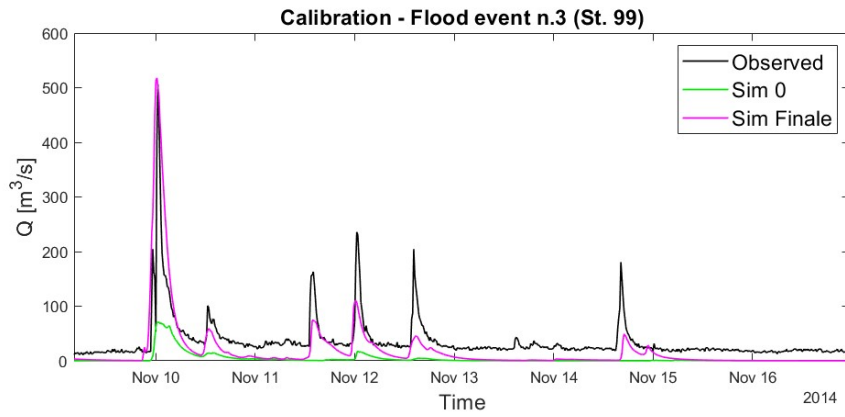


Figure 3.14: Calibration: Flood event n.3.

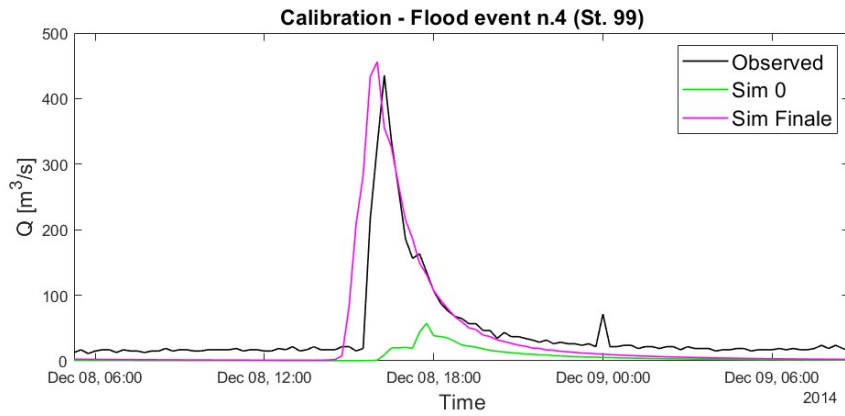


Figure 3.15: Calibration: Flood event n.4.

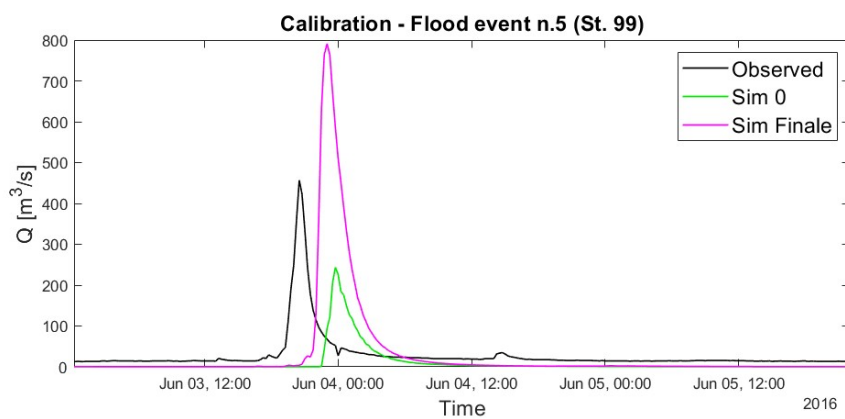


Figure 3.16: Calibration: Flood event n.5.

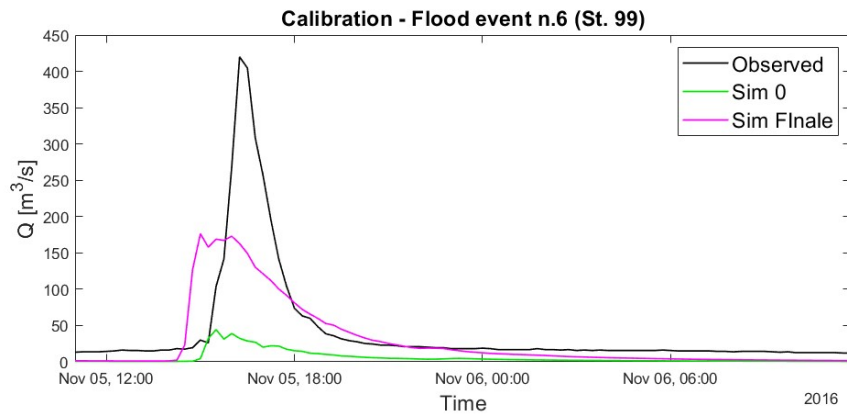


Figure 3.17: Calibration: Flood event n.6.

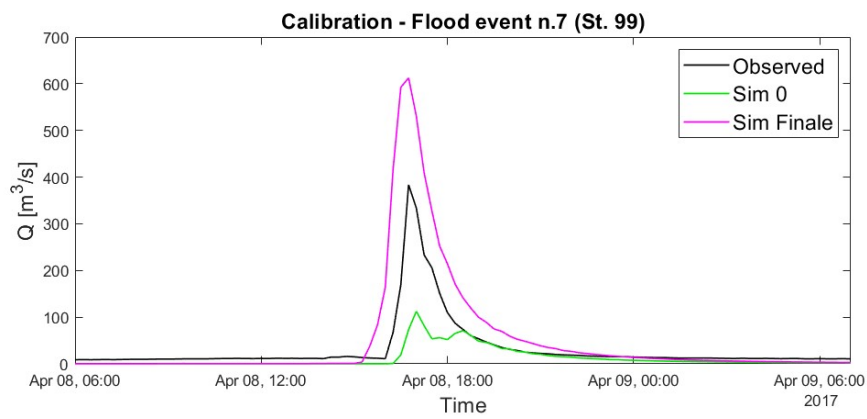


Figure 3.18: Calibration: Flood event n.7.

## Validation

The validation consists of comparing the calculated discharge with the simulated one for a time period different from the one of calibration. This phase is useful to understand if the result of the model can be satisfying also for a data set in which the model has not been calibrated. The period of time considered for this procedure goes from January 2018 to December 2020.

As done for the calibration, also in the validation it is necessary to pick flood events. The chosen ones are:

- Event n.1: started at 05:45 AM on the 18th of February 2019 and ended at 05:15 PM on the 19th of February 2019;
- Event n.2: started at 10:15 PM on the 17th of April 2019 and ended at 08:45 AM on the 8th of April 2019;
- Event n.3: started at 11:30 PM on the 6th of June 2019 and ended at 01:00 AM on the 8th of June 2019;
- Event n.4: started at 06:45 PM on the 10th of March 2020 and ended at 06:00 AM on the 11th of March 2020;
- Event n.5: started at 04:45 PM on the 15th of April 2020 and ended at 06:45 AM on the 16th of April 2020;
- Event n.6: started at 07:45 PM on the 1st of September 2020 and ended at 01:45 AM on the 3rd of September 2020;
- Event n.7: started at 13:15 PM on the 28th of November 2020 and ended at 07:30 AM on the 29th of November 2020.

To understand if the model is acceptable also for this period it's necessary to calculate adaptation indexes previously introduced. From 3.4 it can be seen that the peak discharge relative mean value of the validation is even smaller than the calibration one. This means the model has been well calibrated. In figures 3.19 to 3.25 are reported the observed flow rates and the simulated ones for each flood event analysed in this phase.

	$\varepsilon_{Q_{peak}}$ [%]	RMSE [ $\text{m}^3/\text{s}$ ]	E [-]	$\bar{\varepsilon}$ [ $\text{m}^3/\text{s}$ ]
<b>Calibration (2014-2017)</b>	5.19	54.81	-0.31	-2.61
<b>Validation (2018-2020)</b>	-3.45	42.00	0.38	11.62

Table 3.4: Indexes for validation and calibration

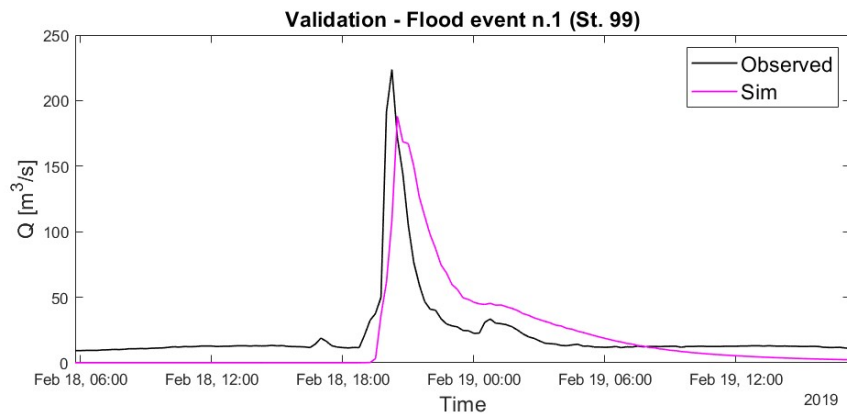


Figure 3.19: Validation: Flood event n.1.

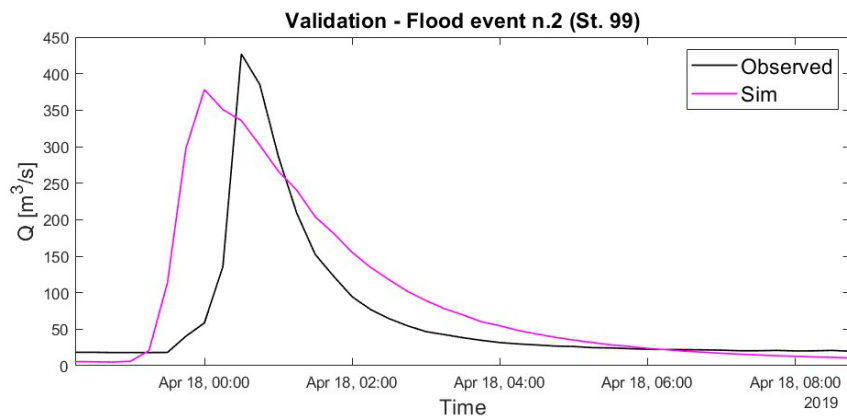


Figure 3.20: Validation: Flood event n.2.

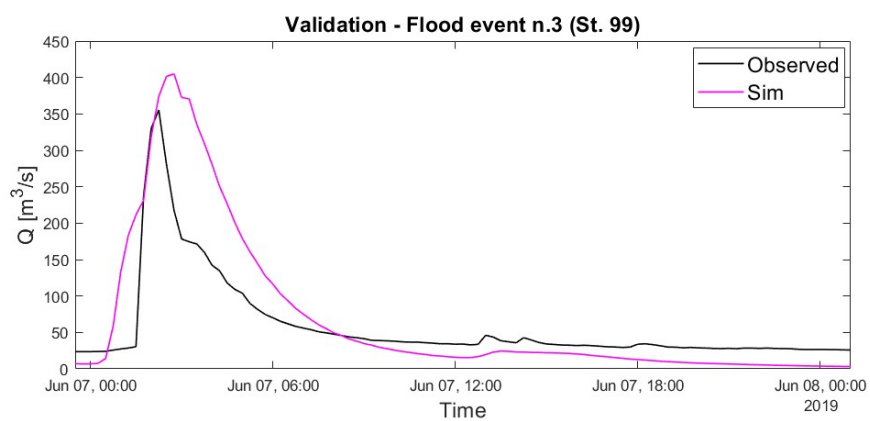


Figure 3.21: Validation: Flood event n.3.

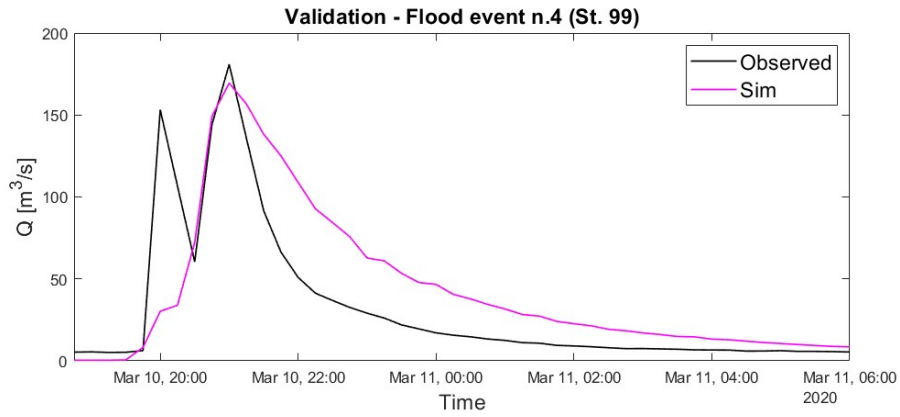


Figure 3.22: Validation: Flood event n.4.

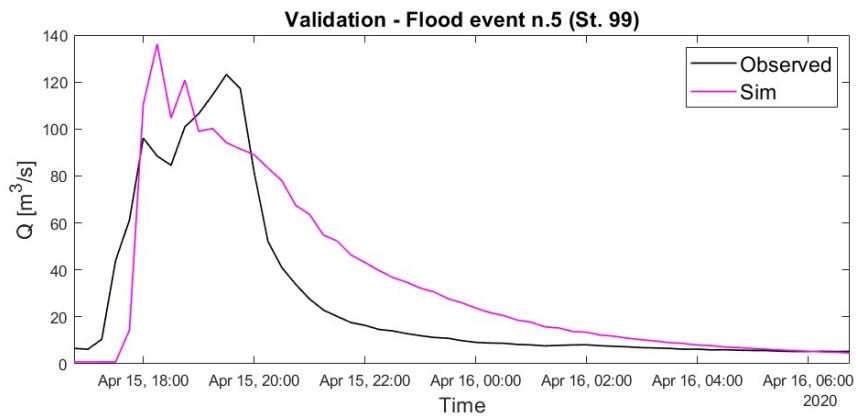


Figure 3.23: Validation: Flood event n.5.

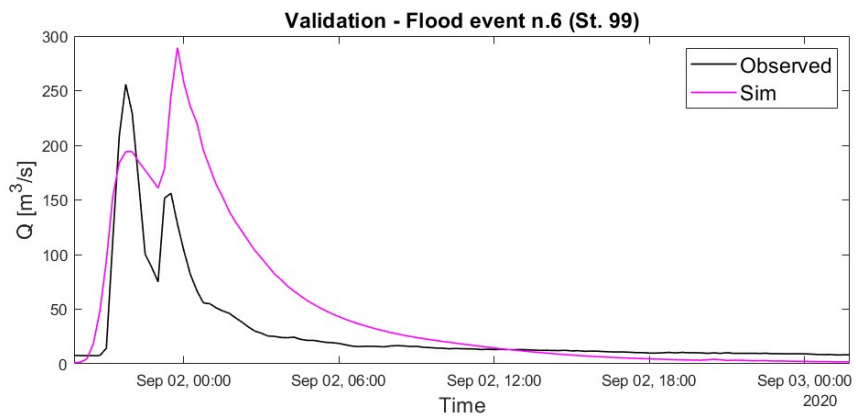


Figure 3.24: Validation: Flood event n.6.

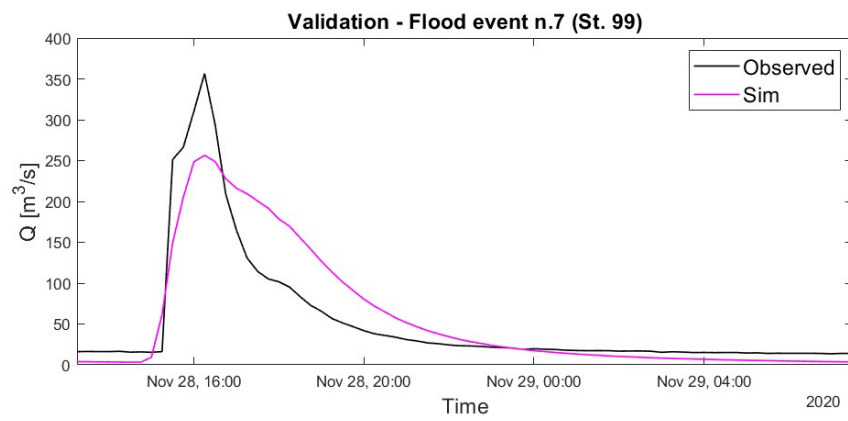


Figure 3.25: Validation: Flood event n.7.



# Chapter 4

## Conclusion

In the present thesis the hydrological FEST model has been applied to the Medellín river basin to evaluate its capability of flood forecasting. The calibration and validation have been carried out through an important network of measurement stations located in the whole basin and developed by SIATA. This procedure allowed to understand whether the hydrological model can be used as a warning system.

A first encouraging result concerns the new orientation given to the computation of the observed flow rates. The choice of estimating the rating curves by the only use of water level data turned out to be a good intuition. As a matter of fact, the discharge time series obtained in this work showed much more realistic and reasonable quantities as compared to the ones computed by (Terbisi, 2021 [1]). This also made it possible to come up with an explanation for two of the river stations investigated, which still displayed extremely high discharge values. It was proven that two hydroelectric power plants, collecting water from outside the river basin and releasing it inside the Medellín catchment area, are the real cause behind those systematically elevated numbers.

Another achievement was the successful calibration performed on a series of single flood events, instead of a cumulative water volume calibration as done by (Terbisi, 2021 [1]). The procedure led, indeed, to well simulated flood events during the calibration as well as in the validation. This means the FEST-WB hydrological model proved to be suitable even for a geographic area with an entirely different meteorological condition with respect to the one in which the model finds its proper application. The Aburrà valley, in fact, is often targeted by precipitation episodes which are very condensed in terms space as well as time.

However, to do this it is fundamental to have a solid network of measures in the examined area, which is rarely available. In this sense, a key role has been played by the significant sensors system of SIATA in the area.

SIATA provided the data used in this work such as: precipitations, temperatures, water depth, water velocity and the surveys of the sections. Recently, they also started to measure other variables, such as wind velocity, air humidity and solar radiation. In the future, when further data will be available, it will be possible to calibrate using more appropriate equations in the FEST-WB model and improving the efficiency of the model.

A next step in this kind of study could be the application of FEST-WB to the other river sections which SIATA can provide water depth data for.

# Bibliography

- [1] Sofia Terbisi. Hydrological modelling of flood forecasting of the Medellín river in Colombia, 2021.
- [2] Juan Pablo Patiño. Diez municipios de antioquia, afectados por las lluvias durante puente festivo, 7 2021. <https://www.elcolombiano.com>.
- [3] M. Werner, J. C. Loaiza, M. C. Rosero Mesa, M. Faneca Sánchez, O. De Keizer, and M. C. Sandoval. Developing Flood Forecasting Capabilities in Colombia (South America). *Flood Forecasting: A Global Perspective*, pages 349–368, 2016.
- [4] SIATA. Sistema de alerta temprana de medellín y el valle de aburrá, 4 2021. [https://siata.gov.co/sitio\\_web/index.php/](https://siata.gov.co/sitio_web/index.php/).
- [5] Stephanie Clark, Ashish Sharma, and Scott A. Sisson. Patterns and comparisons of human-induced changes in river flood impacts in cities. *Hydrology and Earth System Sciences*, 22(3):1793–1810, 2018.
- [6] P. C.D. Milly, R. T. Wetherald, K. A. Dunne, and T. L. Delworth. Increasing risk of great floods in a changing climate. *Nature*, 415(6871):514–517, 2002.
- [7] Sharad Kumar Jain, Pankaj Mani, Sanjay K. Jain, Pavithra Prakash, Vijay P. Singh, Desiree Tullos, Sanjay Kumar, S. P. Agarwal, and A. P. Dimri. A Brief review of flood forecasting techniques and their applications. *International Journal of River Basin Management*, 16(3):329–344, 2018.
- [8] L. Alfieri, P. Burek, E. Dutra, B. Krzeminski, D. Muraro, J. Thielen, and F. Pappenberger. GloFAS-global ensemble streamflow forecasting and flood early warning. *Hydrology and Earth System Sciences*, 17(3):1161–1175, 2013.
- [9] Luc Feyen, Jasper A. Vrugt, Breannán Ó Nualláin, Johan van der Knijff, and Ad De Roo. Parameter optimisation and uncertainty assessment for large-scale streamflow simulation with the LISFLOOD model. *Journal of Hydrology*, 332(3-4):276–289, 2007.

- [10] J. Thielen, J. Bartholmes, M.H. Ramos, and A. de Roo. The European Flood Alert System – Part 1: Concept and development. *Hydrology and Earth System Sciences Discussions*, 5(1):257–287, 2009.
- [11] Efraín Domínguez-Calle and Sergio Lozano-Báez. Estado del arte de los sistemas de alerta temprana en Colombia. *Revista de la Academia Colombiana de Ciencias Exactas, Físicas y Naturales*, 38(148):321, 2014.
- [12] Juan-David López-García, Yesid Carvajal-Escobar, and Angélica-María Enciso-Arango. Sistemas de alerta temprana con enfoque participativo: un desafío para la gestión del riesgo en colombia TT - Early warning systems with a participative approach: a challenge for risk management in colombia. *Rev. luna azul*, (44):231–246, 2017.
- [13] María Alejandra Ochoa Isaza. *Impacto de la información a partir de radar meteorológico en la simulación hidrológica distribuida: simulación de eventos extremos y ventajas para la gestión del riesgo en la cuenca del río Medellín*. PhD thesis, 2013.
- [14] Ministerio de Ambiente y Desarrollo Sostenible (MADS), Corporación Autónoma Regional del Centro de Antioquia (Corantioquia), Área Metropolitana del Valle de Aburrá (AMVA), Corporación Autónoma Regional de las Cuencas de los Ríos Negro y Nare (CORNARE), CPA INGENIERÍA S.A.S, and Fondo Adaptación. Actualización POMCA Río Aburrá. Plan de Ordenación y Manejo de la Cuenca Hidrográfica. page 486, 2019.
- [15] GitHub. *Land Cover (GLCNMO) - Global version*, 04 2021. <https://globalmaps.github.io/glcnm.html>.
- [16] ISRIC. *SoilGrids*, 04 2021. <https://soilgrids.org/>.
- [17] Rubén A. García-Gaines and Susan Frankenstein. USCS and the USDA Soil Classification System. *UPRM and ERDC Educational and Research Internship Program*, (March):37, 2015.
- [18] Oscar Gabriel Cáardenas Hernández. *Segundo levantamiento integrado de cuencas hidrográficas del municipio de Medellín*.
- [19] El colombiano, 5 2021. <https://www.elcolombiano.com>.
- [20] Carlos López. Emergencias por aguacero en medellín, sabaneta y envigado, 6 2021. <https://www.elcolombiano.com>.

- [21] Ferney Arias Jiménez. Aguacero en medellín causa cortes de energía y suspensión en metrocables, 6 2021. <https://www.elcolombiano.com/antioquia/medellin/balance-lluvias-en-medellin-en-navidad-2020-FF14335154>.
- [22] G Ravazzani, D Rabuffetti, C Corbari, and ... Validation of FEST-WB, a continuous water balance distributed model for flood simulation. *31° Convegno Nazionale di Idraulica e Costruzioni Idrauliche*, page 9, 2008.
- [23] C Corbari, J Martinelli, G Ravazzani, and M Mancini. Snow satellite images for calibration of snow dynamic in a continuous distributed hydrological model. *Hydrology and Earth System Sciences Discussions*, 4(6):3979–4004, 2007.
- [24] G Ravazzani, D Rabuffetti, C Corbari, A Ceppi, and M Mancini. Testing FEST-WB, a continuous distributed model for operationa quantitative discharge forse in the upper Po river. *Analyses and images of hydrological extremes mediterranean enviroment*, pages 115–129, 2008.
- [25] Encyclopædia Britannica. Water-cycle, 6 2021. <https://www.britannica.com>.
- [26] Elena Angela Maria Corso. *Stime di precipitazione da satellite della costellazione GPM per la modella zione idrologica del bacino del tanaro*. PhD thesis, 2018.
- [27] R.H. Brooks and A.T. Corey. Verifica di diversi modelli di infiltrazione nella modellistica a. *Physics and Chemistry of Glasses: European Journal of Glass Science and Technology Part B*, 1964.
- [28] Davide Sonvico. *Verifica di diversi modelli di infiltrazione nella modellistica idrologica a scala di bacino in bacini pre alpini e semi-aridi*. PhD thesis, 2017.
- [29] Lijun Su, Quanjiu Wang, Yuyang Shan, and Beibei Zhou. Estimating Soil Saturated Hydraulic Conductivity using the Kostiakov and Philip Infiltration Equations. *Soil Science Society of America Journal*, 80(6):1463–1475, 2016.
- [30] Voltaggio Simone. Infiltrazione, 5 2021. <https://manualedelgeologo.it/infiltrazione/>.
- [31] U Adindu Ruth, K Igbokwe Kelechi, and I Dike Ijeoma. Philip Model Capability to Estimate Infiltration for Solis of Aba , Abia State. 5(2):63–68, 2015.

- [32] Giovanni Ravazzani, Chiara Corbari, Stefano Morella, Paride Gianoli, and Marco Mancini. Modified Hargreaves-Samani Equation for the Assessment of Reference Evapotranspiration in Alpine River Basins. *Journal of Irrigation and Drainage Engineering*, 138(7):592–599, 2012.
- [33] Martin Allen, Richard G., PEREIRA, Luis S., RAES, Dirk and SMITH. FAO Irrigation and Drainage Paper Crop by. *Irrigation and Drainage*, 300(56):300, 1998.
- [34] By George H Hargreaves. Defining and using reference evapotranspiration. *Journal of Irrigation and Drainage Engineering*, 120(6):1132–1139, 1994.
- [35] Nicola Montaldo, Vania Toninelli, John D. Albertson, Marco Mancini, and Peter A. Troch. The effect of background hydrometeorological conditions on the sensitivity of evapotranspiration to model parameters: Analysis with measurements from an Italian alpine catchment. *Hydrology and Earth System Sciences*, 7(6):848–861, 2003.
- [36] N. Montaldo, G. Ravazzani, and M. Mancini. On the prediction of the Toce alpine basin floods with distributed hydrologic models. *www.interscience.wiley.com*, 2274(November 2008):2267–2274, 2007.
- [37] Empresas Pùblicas de Medellín, 2023. <https://cu.epm.com.co/institucional/sobre-epm/nuestras-plantas/plantas-de-energia/centrales-hidroelectricas-epm#Centrales-Generaci-n-516>.

# Appendix A

## HEC-RAS river cross sections

This appendix reports the river cross sections obtained with the software HEC-RAS for each station. Every figure features the water level related to the the maximum discharge bearable by the river geometry.

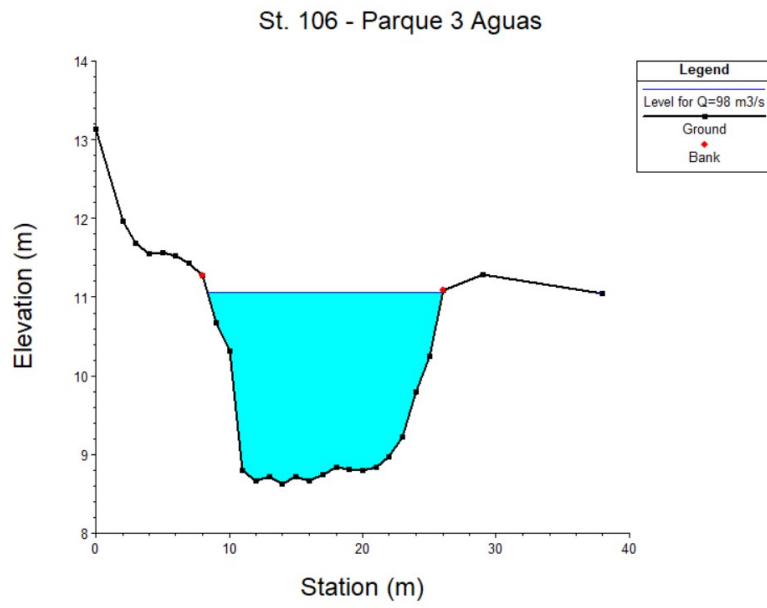


Figure A.1: Parque 3 Aguas cross section.

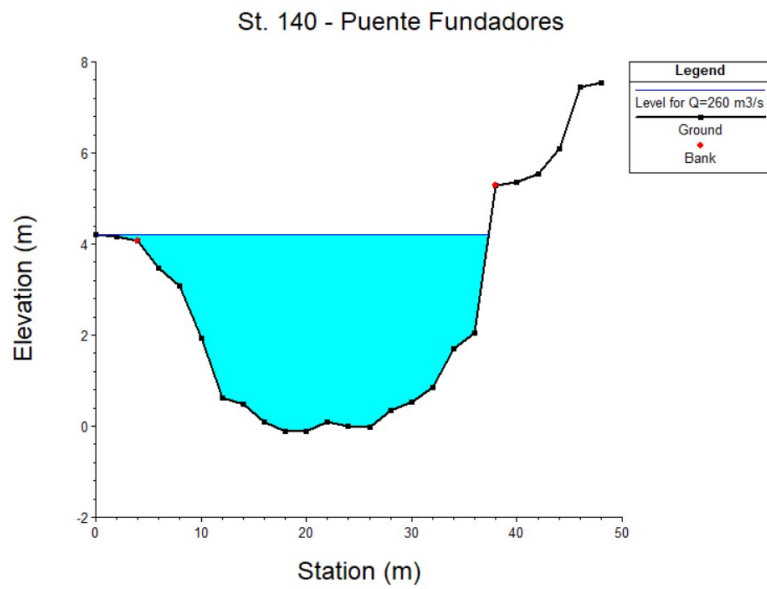


Figure A.2: Puente Fundadores cross section.

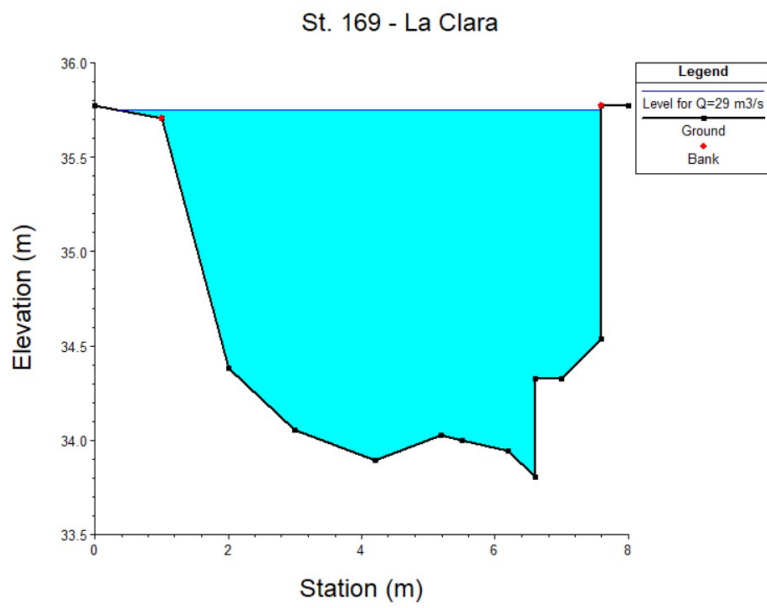


Figure A.3: La Clara cross section.

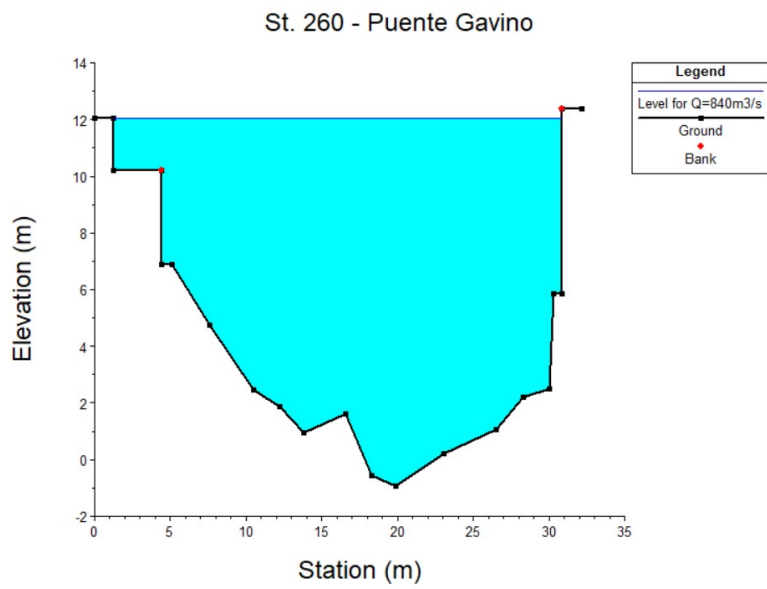


Figure A.4: Puente Gavino cross section.



# Appendix B

## Rating curves

The appendix shows the graphs of the interpolation curve of water depth and discharge.

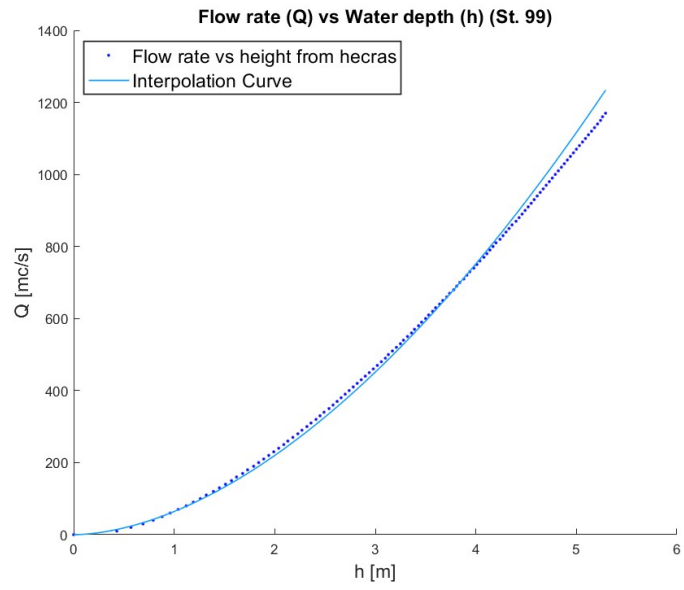


Figure B.1: Rating curve for the section Aula Ambiental.

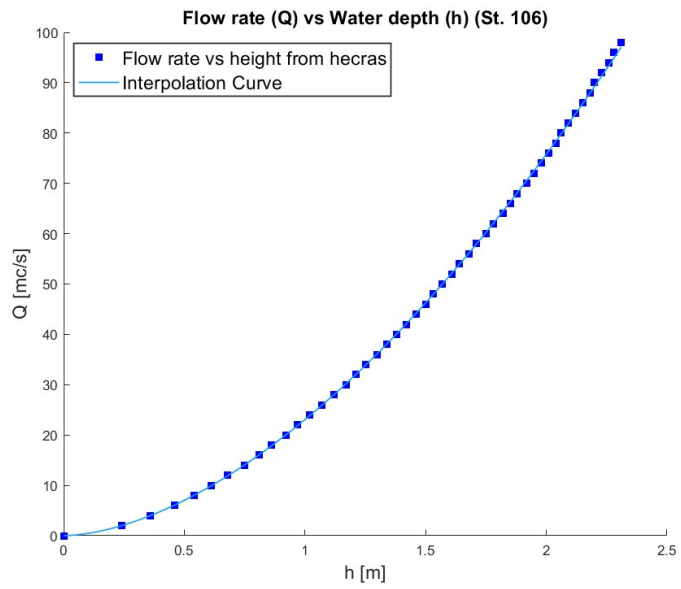


Figure B.2: Rating curve for the section Parque 3 Aguas.

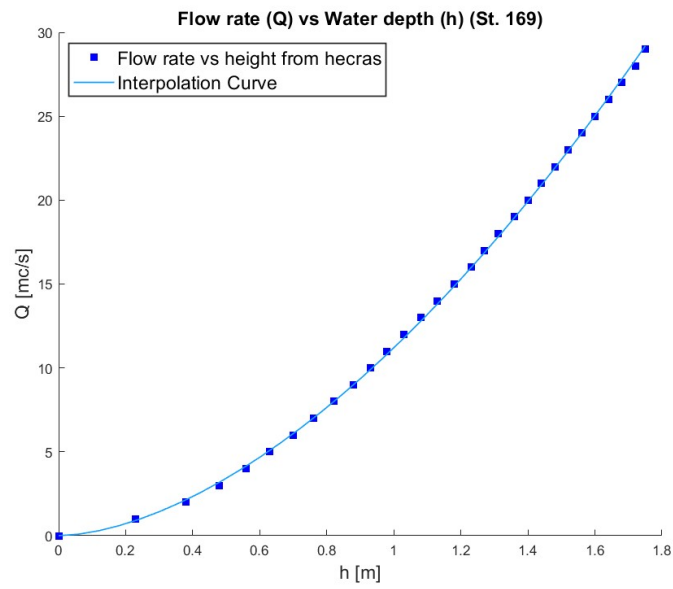


Figure B.3: Rating curve for the section La Clara.

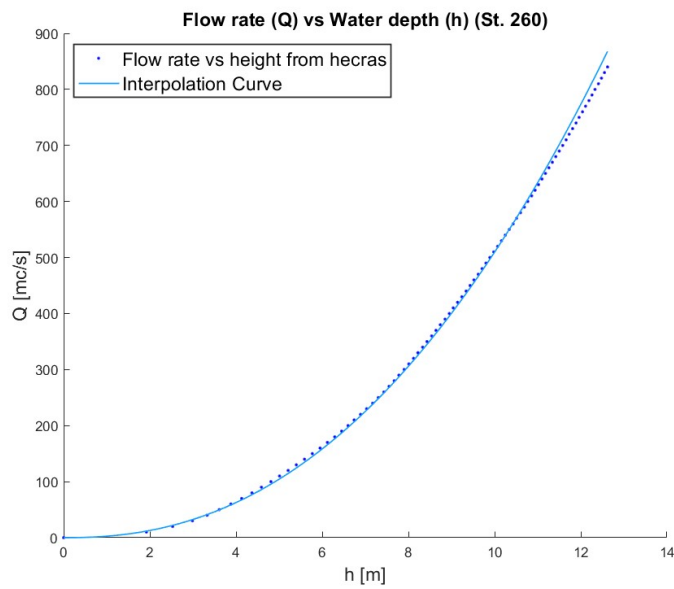


Figure B.4: Rating curve for the section Puente Gavino.



# Ringraziamenti

Al Professor Giovanni Ravazzani va il mio primo ringraziamento. Negli ultimi mesi è stato una presenza rassicurante e una guida dalla gentilezza e comprensione rare. Ringrazio, inoltre, Lisdey Verónica Herrera Gómez per il suo prezioso apporto nell'interpretare al meglio i risultati ottenuti in corso d'opera.

Alla Sofia va certamente il mio grazie più sentito. Non oso immaginare la profondità del baratro in cui mi troverei ora se 10 anni fa' non avessi trovato lei.

Alla Milanie non so come dire grazie. Il primo giorno di università ho sentito che avrei dovuto conoscerla a tutti i costi. Tutti gli altri giorni hanno confermato questa intuizione.

Ringrazio, poi, Luca e Fabio per non avere mai giudicato (credo) la mia ignoranza e per la disponibilità immensa nello spiegarmi i concetti più ovvi.

L'ultimo grazie lo tengo per l'Isabella e la Federica. Le lascio sempre per ultime perchè sanno di essere le prime.

Infine, alla mia famiglia faccio i complimenti per essersi laureati tutti in ingegneria idraulica insieme a me. "Congratulazioni classe 2004. Ce l'abbiamo fatta!". (Cit.)

*"È una giornata memorabile. Per la prima volta dopo sedici anni dormirò bene."*  
M.